Electronic Supplementary Material (ESI) for ChemComm.

-SUPPORTING INFORMATION-

Evaluation of the role of DNA surface for enhancing the activity of scaffolded enzymes

Peng Lin, Huyen Dinh, Yuki Morita, Zhengxiao Zhang, Eiji Nakata, Masahiro Kinoshita, and Takashi Morii*

Contribution from Institute of Advanced Energy, Kyoto University, Uji, Kyoto 611-0011, Japan.

*To whom correspondence should be addressed:

Prof. Takashi Morii

Tel.: +81 774-38-3515

Fax: +81 774-38-3516

E-mail: t-morii@iae.kyoto-u.ac.jp

Table of contents

Materials and Methods

Materials

The single-stranded M13mp18 viral DNA (7249) was purchased from Guild Biosciences. pSNAP-tag (T7)-2 Vector, restriction enzymes (*Nde*I, *Hind*III and *Bam*HI), BG-GLA-NHS (S9151S) and Bovine Serum Albumin (BSA, BS9000S) were purchased from New England Biolabs. pFN18A HaloTag® T7 Flexi® Vector and 5-chlorohexane (CH) derivative (HaloTag Succinimidyl Ester (O2) Ligand (P1691)) were purchased from Promega. Purified DNA origami staple strands, oligonucleotide primers, and all other oligonucleotides were obtained from Sigma-Aldrich (St. Louis, MO), Japan Bio Services Co., LTD (Saitama, Japan) or Thermal Fisher Scientific (Tokyo, Japan). *Escherichia coli* BL21(DE3)pLysS competent cells were purchased from Invitrogen (Carlsbad, CA). *β*-Nicotinamide adenine dinucleotide in reduced (NADH) and oxidized (NAD^+) forms were obtained from Oriental Yeast (Tokyo, Japan). Xylose, xylitol, gel electrophoresis grade acrylamide, bis(acrylamide), phenol, and all other chemicals and reagents were purchased from Wako Chemicals (Tokyo, Japan) or Nacalai Tesque (Kyoto, Japan). Mini Elute Gel Extraction Kit was from QIAGEN (Tokyo, Japan). HisTrap HP column (5 mL), HiTrap SP XL column (5 mL), and Sephacryl S-400 were purchased from GE Healthcare Japan Inc. (Tokyo, Japan). PrimeSTAR HS DNA polymerase, T4 DNA ligase, and *E. coli* DH5α competent cells were obtained from TaKaRa Bio Inc. (Shiga, Japan). Toyopearl HW-55F was purchased from Tosoh Bioscience GmbH (Griesheim, Germany). Ultrafree-MC-DV column was obtained from Merckmillipore (Darmstadt, Germany). Bio-spin® 6 column was purchased from Bio-Rad (Tokyo, Japan). Cosmosil 5C18-MS II column (4.6 mm × 150 mm) was purchased from Nacalai tesque (Kyoto, Japan). Low-binding microtube (BT-150L, 1.5 mL, nonpyrogenic & RNase- / DNase- free) was purchased from Ina OPTIKA CO., LTD (Osaka, Japan).

Preparation of DNA Scaffold

DNA scaffold was prepared by following the previous protocol.[1] A solution (50 μL) containing M13mp18 (20 nM) and staple DNA strands (10 equiv, 200 nM; nucleotide sequences for staple strands were shown in Table S5 and S6) in a DNA scaffold folding buffer (pH 8.0) containing 5 mM Tris, 1 mM EDTA and 8 mM $MgCl_2$, the mixture was subjected to a thermal-annealing ramp for folding with following program: 80 °C to 60 °C at 5 min/°C, 60 °C to 10 °C at 75 min/°C, and finally holding at 10 °C (C1000 Thermal Cycler, Bio-Rad). The sample was then purified by Sephacryl S-400 to remove the excess staple strands. The concentration of DNA scaffold was quantified by the absorbance at 260 nm using the determined extinction coefficient of DNA scaffold (1.20×10^8 $M^{-1}cm^{-1}$) (Note S1).

Construction of an expression vector for HG-XDH

A gene encoding HG-XDH was constructed via overlapping PCR using p4LZ vector containing GCN4-XDH gene[2] and pFN18A HaloTag® T7 Flexi® Vector containing a Halo-tag gene. The primer pairs were shown in Table S7. The PCR products were run on a 1% agarose gel in 1× TAE buffer and purified by a Mini Elute Gel Extraction Kit. The PCR products and pET-30a were digested with *Nde*I and *Bam*HI and were purified in the same manner, separately. These products were incubated with T4 DNA ligase. The mixture was then transformed into *E. coli* DH5α competent cells for amplification. The purity and sequence of vector encoding HG-XDH

(termed as pET-30a-HG-XDH) were checked and transformed into *E. coli* BL21(DE3)pLysS competent cells.

Overexpression and Purification of HG-XDH

The transformed cells were grown at 37 °C until OD_{550} reached 0.45, and protein expression was induced with 1 mM IPTG for 24 h at 18 °C. The soluble fraction of the cell lysate containing HG-XDH was loaded on a HisTrap HP column in 50 mM phosphate buffer (pH 7.5) containing 200 mM NaCl, 1 mM dithiothreitol, and 10 mM xylitol and was eluted by imidazole gradient. The fractions containing HG-XDH were loaded on a HiTrap SP XL column in 20 mM phosphate buffer (pH 7.0) containing 1 mM dithiothreitol and 10 mM xylitol and eluted by NaCl gradient. The purified HG-XDH was dialyzed by using 50 mM phosphate buffer (pH 8.0), containing 0.5 M NaCl, 1 mM dithiothreitol, 2 mM $MgCl_2$, and 10 mM xylitol, and 50% glycerol and stocked at -20 °C. The purity of HG-XDH was checked by SDS-polyacrylamide gel electrophoresis (PAGE). The major band in SDS-PAGE corresponded to the calculated molecular weight of HG-XDH (82046 Da, monomer size) with purity over 95%.

TEM Characterization

DNA scaffold (2 to 3 nM, 2 μL) was placed onto a TEM grid and incubated for 2 minutes, then the extra sample was removed by filter paper. MilliQ water (15 to 20 μL) was used to wash the surface of TEM grid, followed by incubation with 2% phosphotungstic acid (2 μL) for 2 min. The surface was washed by MilliQ water consecutively. Samples were visualized using a TEM microscope (JEOL JEM-2200FS + CETCOR) after the preparation.

Preparation of the DNA Scaffold Assembled with ZS-XR or HG-XDH

DNA scaffolds were constructed either containing the binding sites (hairpin DNA) with BG-GLA-NHS modification for ZS-XR attachment or the binding sites with 5-chlorohexane (CH) derivatives modification for HG-XDH attachment (Table S1). 10 nM DNA scaffold with binding sites was incubated with 200 nM ZS-XR or HG-XDH in a buffer (pH 7.0) containing 40 mM Tris-HCl, 20 mM acetic acid, and 12.5 mM $MgCl_2$, 5 mM β-mecaptoethanol, 0.002% Tween20 and 1 μM $ZnCl_2$ at 4 °C for 1 h. The mixture was purified by gel filtration (500 μL in volume of Toyopearl HW55F) in an Ultrafree-MC-DV column with a buffer (pH 7.0) containing 40 mM Tris-HCl, 20 mM acetic acid, and 12.5 mM $MgCl_2$ to remove the excess amount of unbound proteins.

Methods

AFM Imaging and Statistical Analysis

The sample was deposited on freshly cleaved mica (1.5 mm ϕ) surface and adsorbed for 5 min at ambient temperature, then washed three times with a buffer (pH 7.0) containing 40 mM Tris-HCl, 20 mM acetic acid, and 12.5 mM $MgCl_2$. The sample was scanned in tapping mode using a fast-scanning AFM system (Nano Live Vision, RIBM Co. Ltd., Tsukuba, Japan) with a silicon nitride cantilever (Olympus BL-AC10DS-A2). At least three independent preparations of each sample were analyzed by AFM, and several images were acquired from different regions of the mica surface. The total number of DNA scaffolds corresponded to the well-formed structures observed under AFM. The binding of ZS-XR or HG-XDH was counted for only ZS-XR or HG-XDH bound to the perfectly folded DNA scaffold. The AFM images were shown in Figure S9 and S10, the direct counting result was shown in Table S2. DNA scaffold was constructed with three

binding sites, the loading numbers of ZS-XR ($N_{ZS\text{-}XR}$) or HG-XDH ($N_{HG\text{-}XDH}$) on each DNA scaffold were 2.54 molecules of monomer of ZS-XR or 2.51 molecules of dimer of HG-XDH (Note S1).

Volume analysis of AFM images

For volume analysis, the AFM images were taken by using high-speed AFM system (Nano Live Vision, RIBM Co. Ltd., Tsukuba, Japan) with a silicon nitride cantilever (Olympus BL-AC10DS-A2). The volume of free enzyme XDH or XDH locating outside the DNA scaffold was analyzed by SPIP software (ver. 6.2.8, Image metrology), and the volume value was defined as the volume of all the pixels inside the shape's contour. The volume data were displayed as a histogram plot and fractions were analyzed by means of a nonlinear curve fit by Origin Pro 2018 (ver. 9.5) software. The molecular volumes were converted to the number of enzyme molecules as shown in Note S1.

Estimation of the concentration of DNA scaffolded enzyme

The concentration of DNA scaffold was quantitated by using a NanoDrop spectrophotometer (Thermo Fisher) at 260 nm and calculated by the determined extinction coefficient of DNA scaffold ($\varepsilon_{DNA\ scaffold} = 1.2 \times 10^8\ M^{-1}cm^{-1}$). The concentration of scaffolded enzyme was calculated as followed:

$$[\text{ZS-XR}]\ (\text{nM}) = N_{ZS\text{-}XR} \times \frac{A_{260}}{\varepsilon_{DNA\,scaffold} \times l} \times 10^9$$

$$[\text{HG-XDH}]\ (\text{nM}) = N_{HG\text{-}XDH} \times \frac{A_{260}}{\varepsilon_{DNA\,scaffold} \times l} \times 10^9$$

Where $N_{ZS\text{-}XR}$ or $N_{HG\text{-}XDH}$ is the loading numbers of ZS-XR or HG-XDH bound on the binding sites on the DNA scaffold by the statistical analysis of AFM images ($N_{ZS\text{-}XR} = 2.54$; $N_{HG\text{-}XDH} = 2.51$). A_{260} is the absorbance at 260 nm of the sample after purification, l is the pathlength (1 cm).

Enzyme Assay of ZS-XR

Catalytic activity of ZS-XR was analyzed according to the previously reported methods by measuring the changes of absorbance at 340 nm (25 °C) derived from the oxidation of NADH in an Infinite 200 PRO microplate reader (TECAN).[3] In a typical experiment, a reaction was started with an addition of NADH (300 μM) to a mixture of ZS-XR (5 nM monomer) and xylose (200 mM) in a buffer (pH 7.0) containing 40 mM Tris-HCl, 20 mM acetic acid, 12.5 mM $MgCl_2$, 100 mM NaCl, 1 μM $ZnCl_2$, 5 μM BSA and 0.002% Tween20. Enzyme activities were measured on the microplate (Greiner Microplate, 655901, 96-well, PS, F-bottom (chimney well) clear, non-binding). The turnover frequency was calculated from the initial reaction velocity divided by the concentration of ZS-XR.

Enzyme Assay of HG-XDH

Catalytic activity of HG-XDH was measured by the changes of absorbance at 340 nm (25 °C) derived from the production of NADH in an Infinite 200 PRO microplate reader (TECAN). In a typical experiment, a reaction was started with an addition of NAD^+ (2 mM) to a mixture of HG-XDH (5 nM dimer) and xylitol (300 mM) in a buffer (pH 7.0) containing 40 mM Tris-HCl, 20

mM acetic acid, 12.5 mM $MgCl_2$, 100 mM NaCl, 1 μM $ZnCl_2$, 5 μM BSA and 0.002% Tween20. Enzyme activities were measured on the microplate (Greiner Microplate, 655901, 96-well, PS, F-bottom (chimney well) clear, non-binding). The turnover frequency was calculated from the initial reaction velocity divided by the concentration of HG-XDH.

The effect of $MgCl_2$ and NaCl on enzyme activity

In the enzyme reaction, 12.5 mM $MgCl_2$ was included to stabilize DNA scaffold, and 100 mM NaCl was used for stabilizing enzymes. The effect of $MgCl_2$ and NaCl on enzyme activity was shown in Figure S22.

Measurements of pH profiles of enzymes

Enzyme activities were measured in a 40 mM Good's buffer with different pH (MES, pH 5.5 to 6.5; HEPES, pH 7.0 to 8.0; HEPPS, pH 8.5; CHES, 9.0). The enzyme assay conditions were indicated in the captions of Figure S14 and S15.

Enzyme stability against the pre-incubation time

For the investigation of ZS-XR stability, 6 nM free ZS-XR or scaffolded ZS-XR (sXR) was pre-incubated in the presence of 5 μM BSA and 0.002% Tween20 at 25 °C in the low-binding tube in a buffer (pH 7.0) containing 40 mM Tris-HCl, 20 mM acetic acid and 12.5 mM $MgCl_2$. The enzyme activities were measured at the interval of 15 min with the final enzyme concentration of 2.5 nM (monomer). For the HG-XDH stability, 6 nM free HG-XDH or scaffolded HG-XDH (sXDH) was incubated with 5 μM BSA and 0.002% Tween20 at 25 °C in the low-binding tube in a buffer (pH 7.0) containing 40 mM Tris-HCl, 20 mM acetic acid and 12.5 mM $MgCl_2$. The enzyme activities were measured at the interval of 12 h with the final enzyme concentration of 2.5 nM (dimer). The enzyme activities were measured as described above. To further verify the function of DNA scaffold, the experiments of enzyme stability were also conducted without the addition of BSA and Tween20 during the pre-incubation in the low-binding tube.

Effects of BSA concentration on the residual activity of free HG-XDH against the incubation time

6 nM free HG-XDH was incubated with different concentration of BSA ranging from 0 to 7.5 μM at 25 °C in the low-binding tube in a buffer (pH 7.0) containing 40 mM Tris-HCl, 20 mM acetic acid and 12.5 mM $MgCl_2$. Enzyme activities were measured after 0 h, 0.5 h and 12 h incubation as described above with the final enzyme concentration of 2.5 nM (dimer).

Synthesis of SNARF derivatives

The SNARF derivative (**1**)[4,5] was synthesized by a modified procedure of previous report.[6] The maleimide-modified SNARF derivative (SNARF-mal) was prepared by the following methods.

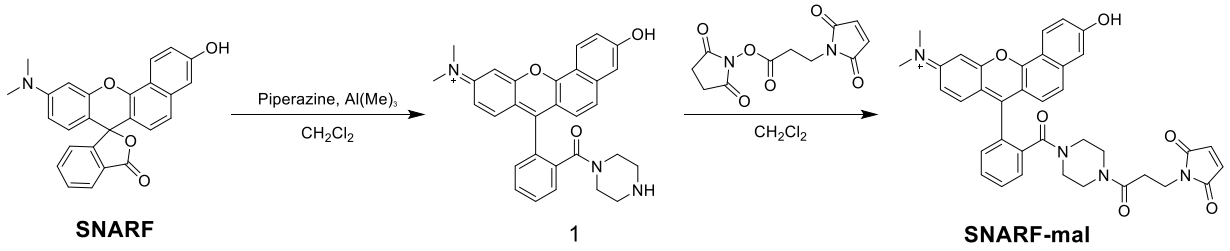

Synthesis of Compound 1[7]

1.4 M trimethylaluminium in hexane (731 μL, 1.02 mmol) was added dropwise into a solution of piperazine (88 mg, 1.28 mmol) in CH_2Cl_2 (5 mL) and the solution was stirred at room temperature. After 1 h, SNARF (104 mg, 0.25 mmol) dissolved in CH_2Cl_2 (20 mL) was added dropwise. After stirring for 2 h under reflux, the reaction solution was placed on ice bath and 0.1 M HCl was added dropwise until no gas was generated. The solution was filtered and the residue was washed twice by CH_2Cl_2 (25 mL) and once by CH_2Cl_2/MeOH (4: 1, 25 mL). The filtrate was concentrated and the residue was dissolved in CH_2Cl_2, the mixture was then filtered to remove insoluble salts and concentrated again. The resulting solid was dissolved in chloroform and washed by water. After concentration, the crude products were purified by column chromatography on amino-bonded silica gel ($CHCl_3$/MeOH: a linear gradient from 1: 0 to 10: 1 (*v/v*)) to give compound **1** in 48% yield (58 mg). ^{1}H NMR (600 MHz; DMSO): δ 8.72 (d, 1H, J_H = 9.0 Hz, Ar-H), 7.75 - 7.64 (m, 4H, Ar-H), 7.52 (d, 1H, J_H = 9.1 Hz, Ar-H), 7.37 - 7.28 (m, 5H, Ar-H), 7.09 (d, 1H, J_H = 9.0 Hz, Ar-H), 3.63 (s, 2H, CH_2), 3.32 - 3.27 (m, 8H, CH_2 and 2(CH_3)), 2.99 (s, 2H, CH_2), 2.84 (s, 2H, CH_2). ESI-TOF-MS *m/z* = 478.17 $[M+H]^+$ (calcd. for $C_{30}H_{28}N_3O_3$, 478.21).

Synthesis of SNARF-mal

Compound **1** (30 mg, 0.06 mmol) was dissolved in CH_2Cl_2 (5 mL). *N*-Succinimidyl 3-maleimidopropionate (33 mg, 0.12 mmol) and trimethylamine (18 μL, 0.12 mmol) were added to the solution. After stirring for 2 h, CH_2Cl_2 was removed and the crude was purified by a reverse phase column chromatography (ODS, H_2O/MeOH: a linear gradient from 9: 1 to 1: 9 (*v/v*)), then by HPLC (column: ULTRON VX-ODS ODS 20 mm × 150 mm / mobile phase 0.05% TFA with 33% to 45% acetonitrile) to give SNARF-mal in 17% yield (6.5 mg). ^{1}H NMR (600 MHz; Acetone-d6): δ 8.57 (d, 2H, J_H = 9.0 Hz, Ar-H), 7.71 - 7.68 (m, 3H, Ar-H), 7.59 (s, 1H, Ar-H), 7.52 (t, 1H, J_H = 4.5 Hz, Ar-H), 7.45 - 7.37 (m, 5H, Ar-H), 7.16 (d, 1H, J_H = 8.9 Hz, Ar-H), 6.70 (s, 2H, CH=CH), 3.52 - 3.16 (m, 16H, 5(CH_2), N(CH_3)$_2$), 2.45 (s, 2H, CH_2). ESI-TOF-MS *m/z* = 629.19 $[M+H]^+$ (calcd. for $C_{37}H_{33}N_4O_6$, 629.24).

Prepraration of ODN-SNARF

Tris(2-carboxyethyl) phosphine (TCEP) was used to deprotect a thiol-modified oligo DNA (ODN-thiol, the sequence was shown in Table S3) at 30 °C for 1 h, then the mixture was first purified by the Bio-spin® 6 column with 50 mM PB buffer (pH 6.5), the concentration of oligo was measured by Nanodrop at 260 nm using the extinction coefficient (189600 $M^{-1}cm^{-1}$) of ODN-thiol. A coupling reaction between deprotected ODN-thiol and SNARF-mal was carried out by incubating ODN-thiol (100 μM) with SNARF-mal (500 μM) at 30 °C for overnight. Firstly, the reaction mixture was purified by Bio-spin® 6 column with 50 mM PB buffer (pH 8.0). Then, ODN-SNARF was purified by reversed-phase HPLC on a Cosmosil 5C18-MS II column (4.6 mm × 150 mm, elution with 100 mM triethylammonium acetate buffer, pH 7.0, linear gradient over 25 min from 30% to 80% acetonitrile at flow rate of 1.0 mL/min). ODN-SNARF was characterized by MALDI-TOF mass spectrometry (AXIMA-LNR, Shimadzu, HPA matrix). ODN-SNARF *m/z* calcd 6960, found 6960.

Preparation of sSNARF-n and sSNARF-f

ODN-SNARF was used for the further conjugation with DNA scaffold via hybridization with the protruding complementary sequence (Figure S2, Table S3 and S4). DNA scaffold was designed with 9 attachment sites (protruding single strand DNA) for the hybridization of the above prepared ODN-SNARF. In brief, ODN-SNARF was included at a molar ratio of 1: 1.2 (SNARF binding sites: ODN-SNARF) in the annealing process of DNA scaffold for the hybridization.

Preparation of SNARF-mal-ME

SNARF-mal (200 μM) was reacted with 2-mercaptoethanol (200 μM) at 30 °C for 1 h in a 40 mM PB buffer (pH 6.5). The purity of SNARF-mal-ME was checked by reversed-phase HPLC with estimated purity of over 90%. SNARF-mal-ME was characterized by ESI-TOF-MS, SNARF-mal-ME *m/z* = 707.23 $[M+H]^+$ (calcd. for $C_{39}H_{38}N_4O_7S$, 706.81).

pH titration and fluorescence spectra measurement

Fluorescence spectra were measured by TECAN Infinite M Nano$^+$ by excitation at 534 nm in the 40 mM acetate, MES, HEPES or CHES buffer (pH 4.6 to 9.5). Fluorescence measurements were performed in the 96-plate (Greiner Microplate, 655906, 96-well, PS, F-bottom (chimney well) μCLEAR®, black, non-binding).

pK_a values of SNARF-mal-ME, sSNARF-n and sSNARF-f

The dual-emission pH indicator follows a sigmoidal function described by equation (1).[8]

$$R = R_{min} + \frac{(R_{max} - R_{min})}{1 + 10^{\mathrm{p}K_a - \mathrm{p}H}} \qquad (1)$$

Where R is the ratio of fluorescence emission intensity at 600 nm over 652 nm (excited at 534 nm), R_{min} is the minimum ratio value (the ratio for the fully protonated form), R_{max} is the maximum ratio value (the ratio for the fully deprotonated form). The curves were fitted by Origin Pro 2018 (ver. 9.5) software using equation (1).

Note S1. Estimation the concentration of DNA scaffold and scaffolded enzyme

Estimation the concentration of DNA scaffold

DNA scaffold was prepared as described in Materials and Methods. The molar absorbance coefficient of DNA scaffold was determined as described previously.[3] The recovery yield of DNA scaffold after gel filtration was deduced by quantification of DNA in the agarose gel electrophoresis band (Figure S21) by following this equation:

$$\text{Recovery yield (\%)} = \frac{band\ intensity_{\ (after\ purification)}}{band\ intensity_{\ (before\ purification)}}$$

The recovery yield of DNA scaffold was 82%, from the starting concentration of DNA scaffold (20 nM), the concentration of DNA scaffold after the purification process was calculated to be 16.4 nM. From the absorbance spectrum of purified DNA scaffold measured by Nanodrop (Thermo Fisher Scientific Inc.), the average molar absorbance coefficient of DNA scaffold at 260 nm was determined (ε = 1.20 × 10^8 M^{-1} cm^{-1}) (average of three independent experiments). The determined molar extinction coefficient is consistent with that of a fully double-stranded M13mp18 molecules (the calculated molar absorbance coefficient is 1.17 × 10^8 M^{-1} cm^{-1} from the website http:// www.molbiotools.com/dnacalculator.html).

Estimation the numbers of ZS-XR or HG-XDH bound on DNA scaffold by counting the protein on the AFM images

The AFM images of scaffolded ZS-XR and scaffolded HG-XDH were shown in Figure S9 and Figure S10, respectively, the counting result was shown in Table S2. The total number of DNA scaffolds corresponded to the well-formed structures observed under AFM. The binding of ZS-XR or HG-XDH was counted only for ZS-XR or HG-XDH bound to the perfectly folded DNA scaffold (Figure S9 and Figure S10). The quantification of enzyme binding numbers was conducted for each set of the freshly prepared enzyme assembly. A typical data is shown below:

In the case of scaffolded ZS-XR, 253 well-formed DNA scaffolds were counted, in which DNA scaffolds with three molecules of ZS-XR (monomer) were 187 (73.9%), DNA scaffolds with two molecules of ZS-XR (monomer) were 28 (11.1%), DNA scaffolds with one molecule of ZS-XR (monomer) were 26 (10.3%), and empty DNA scaffolds were 12 (4.7%). The counting results indicated that 95.3% of DNA scaffolds were occupied with ZS-XR ($P_{ZS\text{-}XR}$ = 95.3%). The average assembly numbers of ZS-XR on DNA was calculated as follow:

$N_{ZS\text{-}XR}$ = 3 × 73.9% + 2 × 11.1% + 1 × 10.3% + 0 × 4.7% = 2.54 (molecules of ZS-XR monomer on each DNA scaffold)

In the case of scaffolded HG-XDH, 376 well-formed DNA scaffolds were counted, in which DNA scaffolds with three molecules of HG-XDH (dimer) were 295 (78.4%), DNA scaffolds with two molecules of HG-XDH (dimer) were 22 (5.8%), DNA scaffolds with one molecule of HG-XDH (dimer) were 16 (4.2%), and empty DNA scaffolds were 43 (11.4%). The counting results indicated that 88.4% of DNA scaffolds were occupied with HG-XDH ($P_{HG\text{-}XDH}$ = 88.4%). The average assembly yield of HG-XDH on DNA was calculated as follow:

$N_{HG\text{-}XDH}$ = 3 × 78.4% + 2 × 5.8% + 1 × 4.2% + 0 × 11.4% = 2.51 (molecules of HG-XDH dimer on each DNA scaffold)

Verification of HG-XDH assembly yield on DNA scaffold by volume analysis

To confirm the assembly yield of HG-XDH on DNA scaffold from the counting results, volume analysis of AFM images was conducted as previously described.[3] It was observed that the AFM cantilever deformed the modular adaptor Halo-GCN4 and enzyme XDH during the analysis with the plausible XDH domain locating outside DNA scaffold. Therefore, volume analysis was conducted only for the plausible XDH domain exsisting next to the DNA scaffold. Firstly, free enzyme XDH was independently characterized by AFM and volume analysis was performed (Figure S10b and Figure S10c), the frequency distribution of molecule volumes of XDH showed that the volume of one dimer of XDH was 260 ± 127 nm^3 (Figure S10d).

Typical AFM images of scaffolded HG-XDH and the volume analysis process were shown in Figure S10e and Figure S10f, the frequency distribution of molecule volume showed three fractions centered at 408 ± 110 nm^3 (30%), 715 ± 212 nm^3 (55%) and 1300 ± 275 nm^3 (15%), respectively, which corresponded to two dimers, three dimers and four dimers of XDH, respectively. On average, 2.85 dimers of XDH were loaded on each DNA scaffold (2 × 15% + 3 × 55% + 4 × 15% = 2.85), which derived from the volume analysis of DNA scaffold bound with proteins. Considering 88.4% DNA scaffolds were observed to bind with HG-XDH ($P_{HG\text{-}XDH}$ = 88.4%) (Table S2), the actual number of bound HG-XDH was calculated as follow:

$N'_{HG\text{-}XDH}$ = 88.4% × 2.85 = 2.519 (molecules of HG-XDH dimer on each DNA scaffold)

This value is well consistent with that derived from the results obtained by direct counting.

Estimation of the concentration of DNA scaffolded enzyme

The molar absorbance coefficient of ZS-XR and HG-XDH at 260 nm were negligible to the value of DNA scaffold alone. Therefore, the concentration of DNA scaffolded enzyme after purification was determined by using the molar absorbance coefficient of DNA scaffold (ε = 1.20 × 10^8 M^{-1} cm^{-1}). The concentration of scaffolded enzyme was calculated as follows:

$$[\text{ZS-XR}]\ (\text{nM}) = N_{\text{ZS-XR}} \times \frac{A_{260}}{\varepsilon_{DNA\,scaffold} \times l} \times 10^9$$

$$[\text{HG-XDH}]\ (\text{nM}) = N_{\text{HG-XDH}} \times \frac{A_{260}}{\varepsilon_{DNA\,scaffold} \times l} \times 10^9$$

where $N_{ZS\text{-}XR}$ or $N_{HG\text{-}XDH}$ is the loading numbers of ZS-XR or HG-XDH bound on the binding sites on the DNA scaffold by the statistical analysis of AFM images ($N_{ZS\text{-}XR}$ = 2.54; $N_{HG\text{-}XDH}$ = 2.51). A_{260} is the absorbance at 260 nm of the sample after purification, l is the pathlength (1 cm).

Note S2. Fitting of pH titration curve of SNARF derivative and estimation of local pH

Fitting of pH titration curve of SNARF derivative

The fluorescence emission spectra were obtained by excitation at 534 nm in the buffer with pH ranging from 4.6 to 9.5. The spectra exhibited fluorescence emission peaks at 600 nm and 652 nm. The ratio of fluorescence intensity at 600 nm over 652 nm upon excitation at 534 nm was taken to plot the pH titration curves against the buffer pH values. The large error bars in the acidic region (Figure 2c and S13) were resulted from the weak and fluctuated fluorescence intensities at 652 nm in the acidic condition (pH 4.6, 5.1 and 5.9) (Figure 2b and S13). SNARF-mal-ME displayed lower ratio value at pH 4.6 compared with sSNARF-n and sSNARF-f. In the curve fitting by Origin, the maximum ratio was fixed to the same value (R_{max} = 1.9). The pK_a values of SNARF-mal-ME, sSNARF-n and sSNARF-f were 6.3 ± 0.1, 7.1 ± 0.1 and 6.8 ± 0.1, respectively.

Estimation of local pH

The local pH near the surface or near the enzyme loaded position in the buffer (pH 7.0) was estimated by following methods.

For the local pH near the DNA scaffold surface, substitution of the estimated pK_a value of 7.1 for the SNARF derivative (sSNARF-n) and the pH of bulk solution (pH 7.0) to the equation (1) (Experimental methods) gave a ratio value (R = 1.113). This ratio value was then substituted to the above equation with the pK_a value of SNARF-mal-ME (6.3) to estimate the local pH near the DNA scaffold surface. The estimated pH at the location of sSNARF-f was obtained in a similar manner using the pK_a value of 6.8.

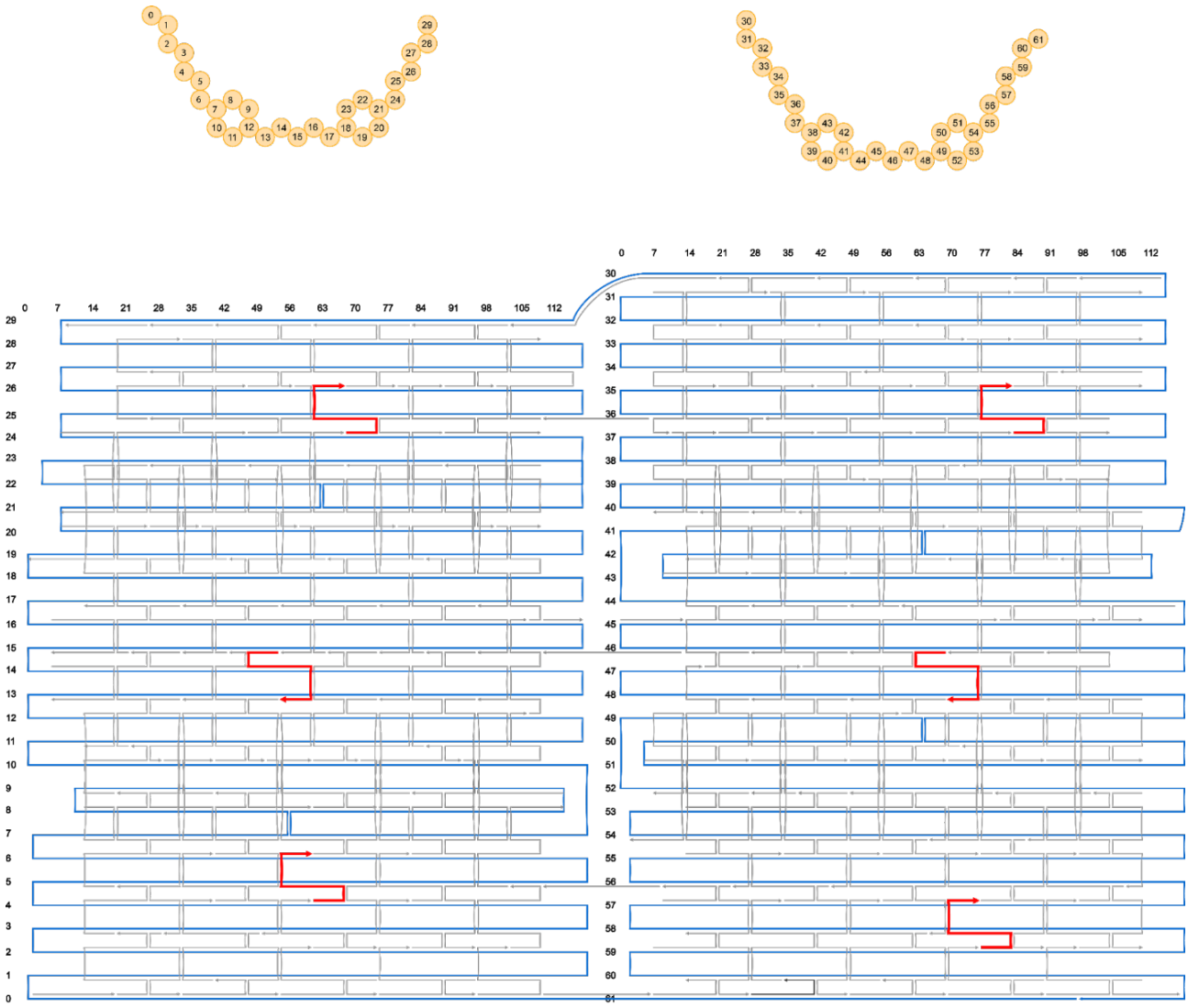

Figure S1. Front view and blueprint modified from caDNAno[9] software interface of DNA scaffold (http://cadnano.org/). The staple strands shown in red represent the binding sites of enzymes.

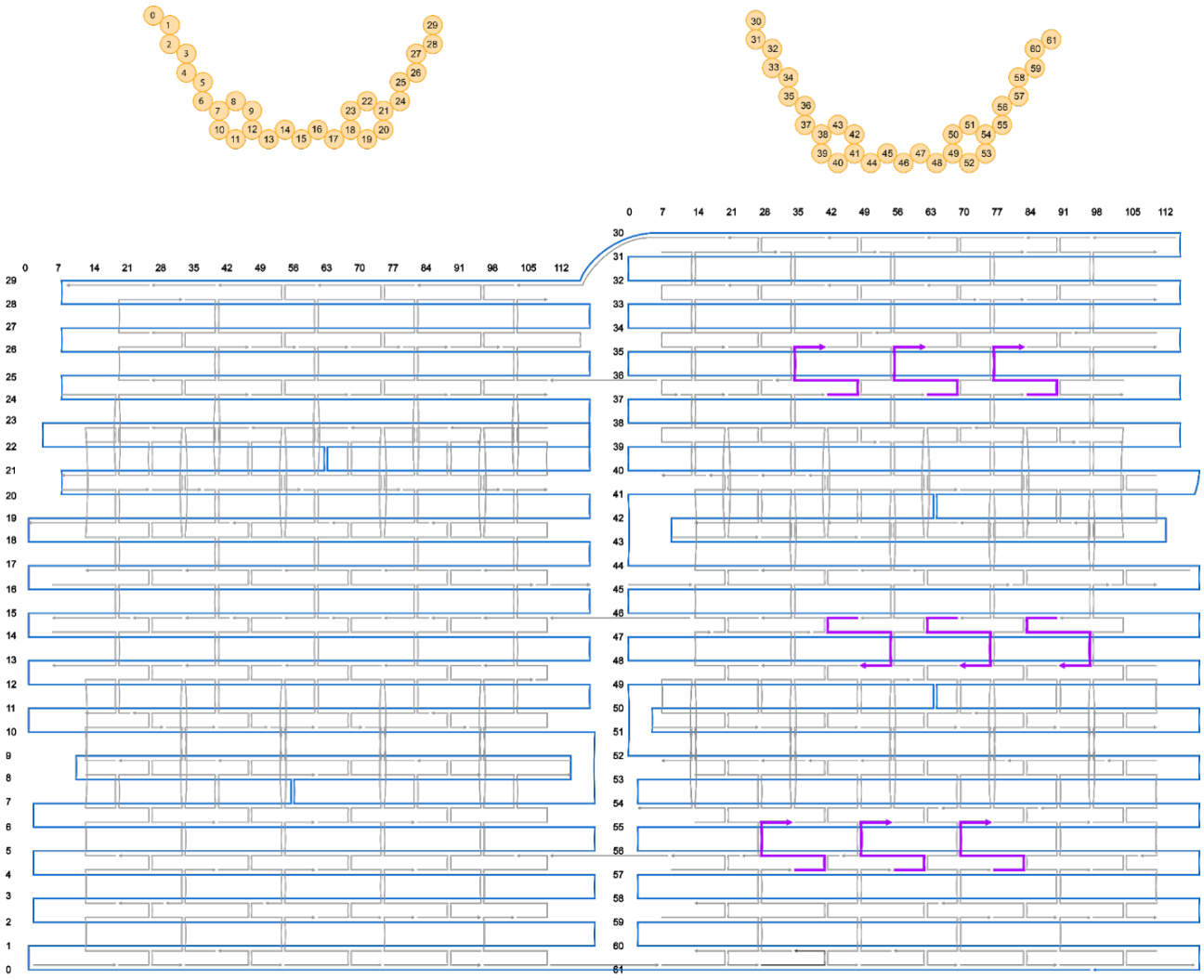

Figure S2. Blueprint modified from caDNAno[9] software interface of DNA scaffold (http://cadnano.org/). The staple strands shown in purple represent the hybridization sites of ODN-SNARF.

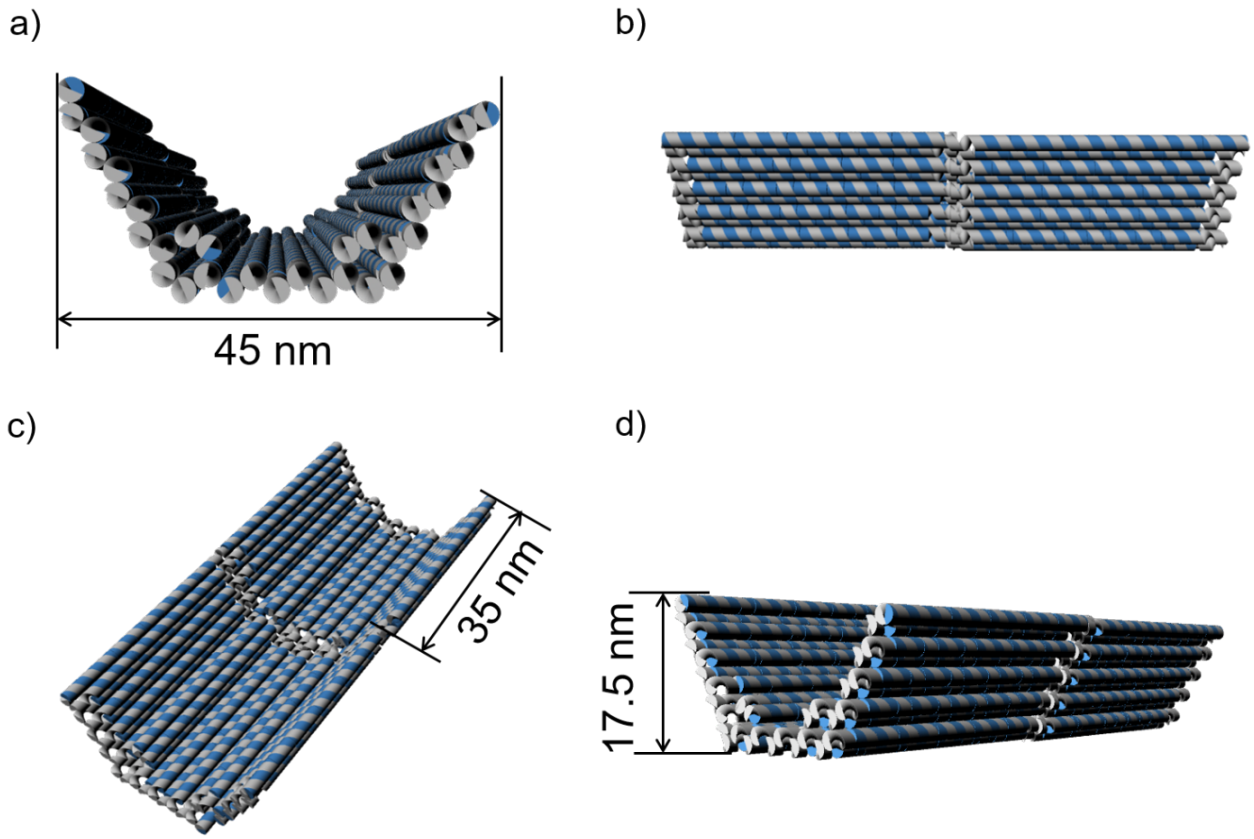

Figure S3. DNA scaffold in different views. (a) Front view, (b) side view, (c) top view and (d) side view. Scaffold model was constructed by using Autodesk Maya (Autodesk® Maya® 2015, student version).

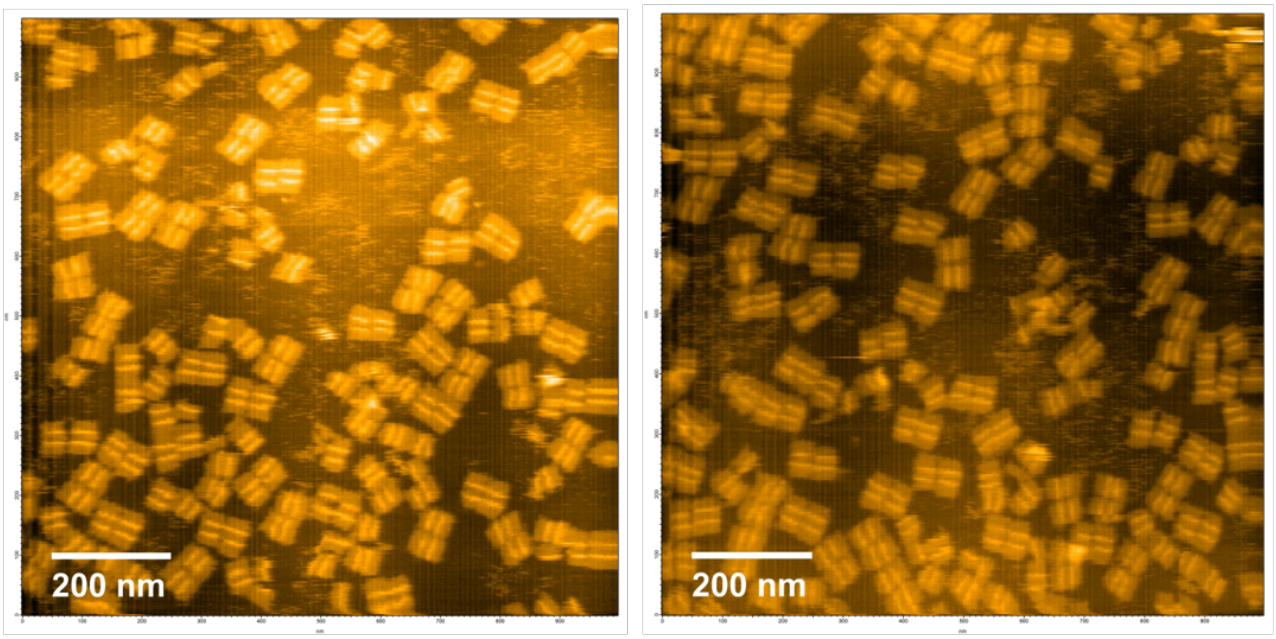

Figure S4. AFM images of DNA scaffold (scale bar: 200 nm). The yield of well-formed DNA scaffold was estimated to be 94% (282/300).

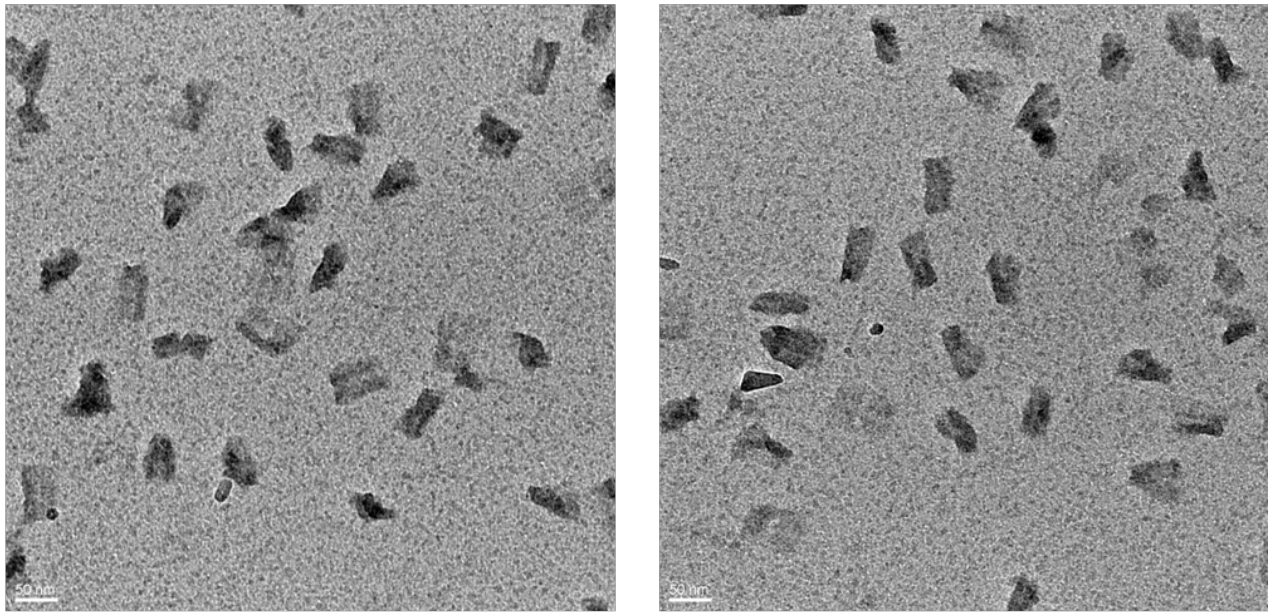

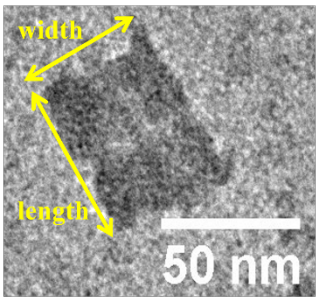

Length: 66.3 ± 4.2 nm
Width: 45.2 ± 3.5 nm

Figure S5. TEM images of DNA scaffold (scale bar: 50 nm). The measured long and narrow sides were 66.3 ± 4.2 nm and 45.2 ± 3.5 nm, respectively, which were well consistent with the designed dimensions. Some unrecognized structures appeared in the images, which most likely formed during the negative staining procedure used for TEM imaging, resulting in structural distortion or collapse of the macromolecular assemblies caused by the air-drying and imaging of conventional specimens under the vacuum conditions of TEM.[10]

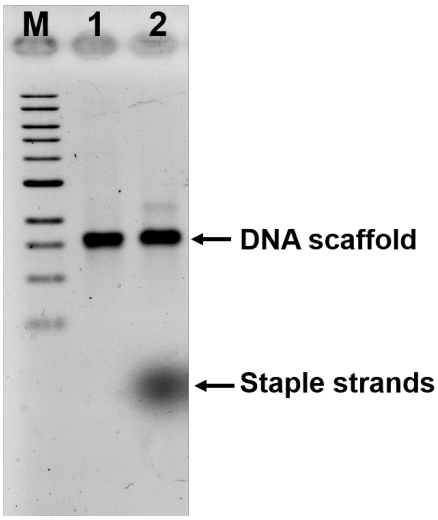

Figure S6. Agarose gel electrophoretic analysis of the DNA scaffold. The gel was stained with ethidium bromide (EtBr) and visualized by using Molecular Imager FX pro (Biorad). Lane M: 1 kb DNA marker, Lane 1: single strand DNA (M13mp18), Lane 2: DNA scaffold. Gel electrophoresis conditions: 1% agarose in 1 × TAE buffer with 12.5 mM $MgCl_2$, 50 V, 6 h.

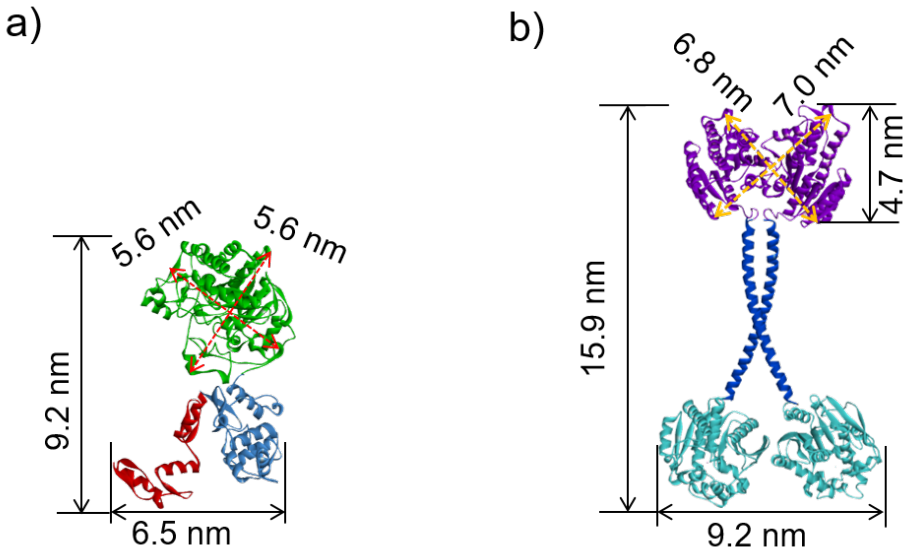

Figure S7. Molecular models of ZS-XR and HG-XDH. (a) A molecular model for enzyme ZS-XR consisting of zif268 (PDB ID: 1ZAA), SNAP-tag (PDB ID: 3KZY), and XR (PDB ID: 3TJL).[3] (b) A molecular model for HG-XDH consisting of GCN4 (PDB ID: 1DGC), Halo-tag (PDB ID: 1CQW), and XDH (PDB ID: 1ZEM). Molecular models were constructed by using Discovery Studio (version 3.1, Accelrys Inc.).

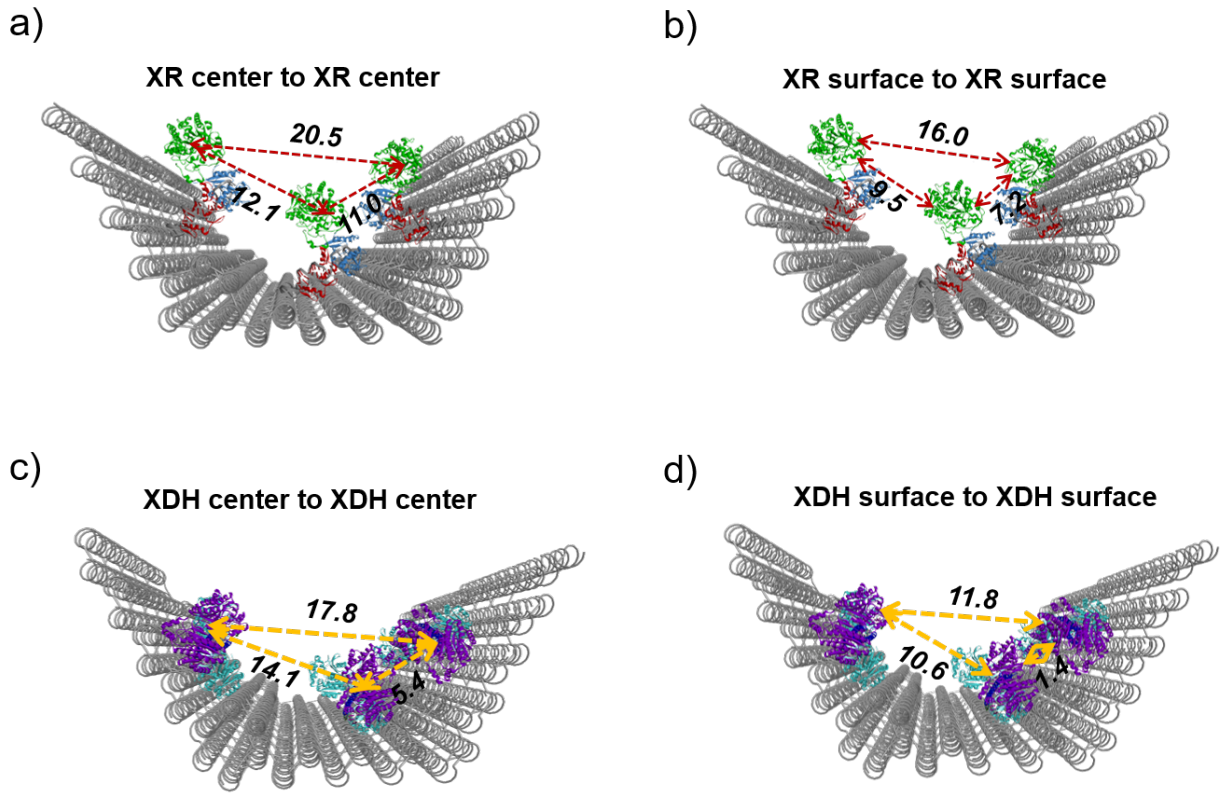

Figure S8. Inter-enzyme distances of scaffolded enzymes. (a) The inter-enzyme distances of XR (center) to XR (center) were 20.5 nm, 12.1 nm and 11.0 nm, respectively. (b) The inter-enzyme distances of XR (surface) to XR (surface) were 16.0 nm, 9.5 nm and 7.2 nm, respectively. (c) The inter-enzyme distances of XDH (center) to XDH (center) were 17.8 nm, 14.1 nm and 5.4 nm, respectively. (d) The inter-enzyme distances of XDH (surface) to XDH (surface) were 11.8 nm, 10.6 nm and 1.4 nm, respectively. The distances were measured by BIOVIA Discovery Studio (version 3.1, Accelrys Inc.).

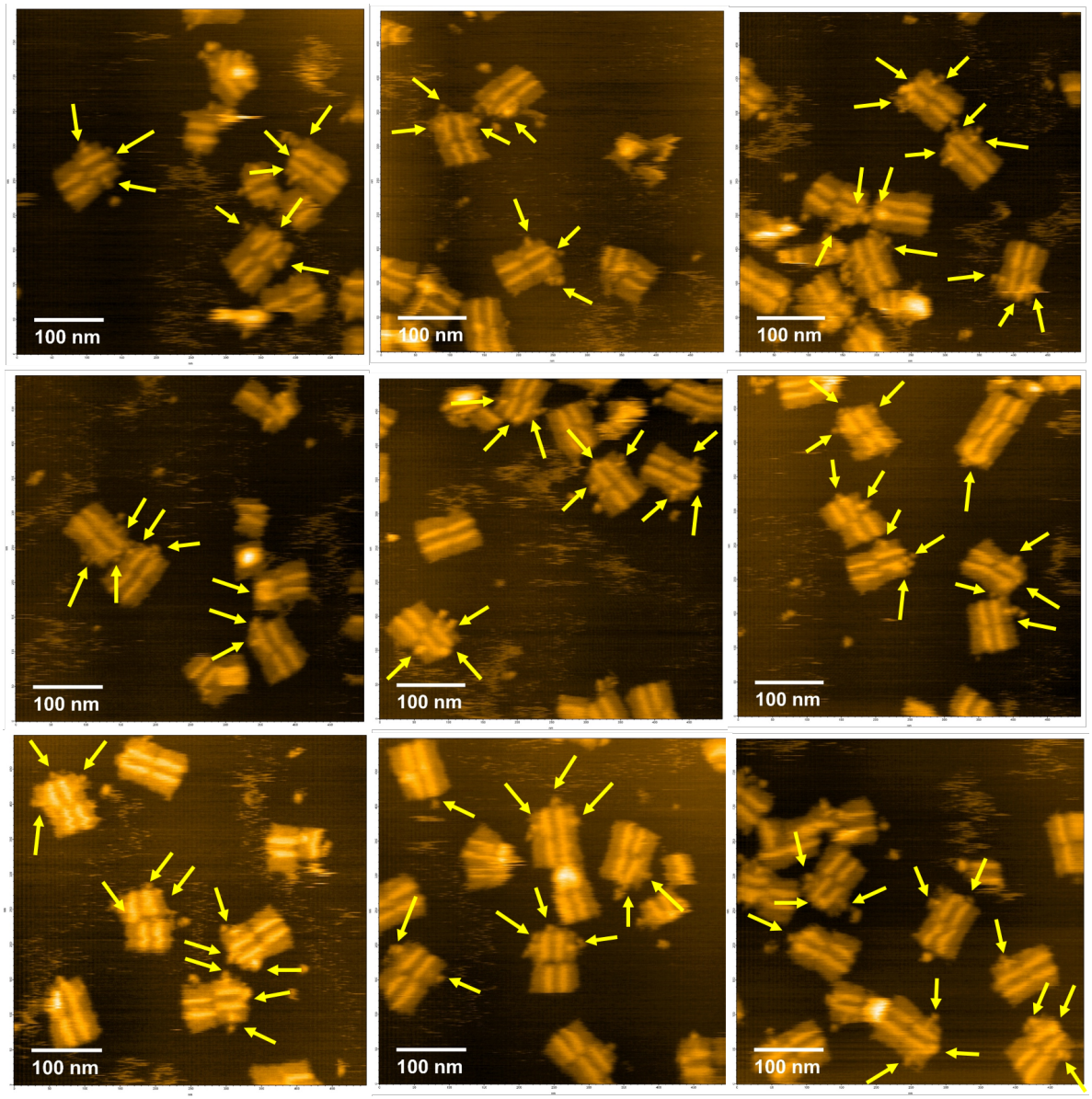

Figure S9. AFM images of ZS-XR assembled on the DNA scaffold with three binding sites (sXR), scale bar: 100 nm. The arrows indicate ZS-XR. An average number of ZS-XR bound to each DNA scaffold was estimated to be 2.54 molecules (253 well-formed DNA scaffolds were counted as shown in Table S2 in supporting information).

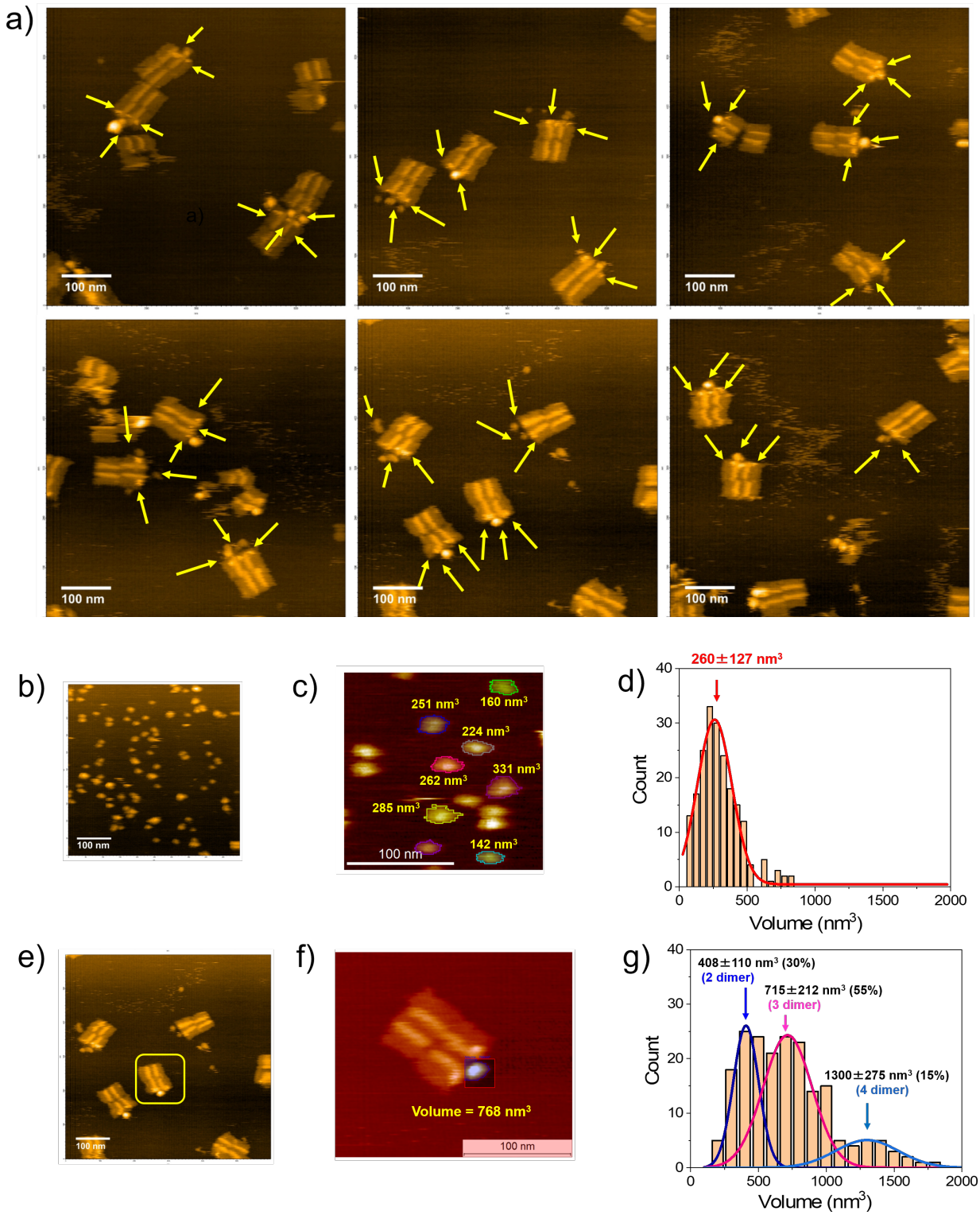

Figure S10. AFM images of HG-XDH assembled on the DNA scaffold with three binding sites (sXDH) and volume analysis. (a) AFM images of HG-XDH assembled on DNA scaffold, scale bar: 100 nm. The arrows indicated the enzyme HG-XDH. An average number of HG-XDH bound to each DNA scaffold was estimated to be 2.51 molecules (376 well-formed DNA

scaffolds were counted as shown in Table S2 in supporting information). (b) AFM image of free enzyme XDH, scale bar: 100 nm. (c) Volume analysis of free enzyme XDH. (d) Frequency distribution of free XDH volume (215 particles were counted), the volume of XDH (dimer) was estimated to be 260 ± 127 nm^3. (e) Typical AFM image of scaffolded HG-XDH (sXDH), scale bar: 100 nm. (f) On the AFM analysis of sXDH, a plausible XDH protion of HG-XDH tended to locate near the outside of scaffold, while modular adaptor Halo-GCN4 of HG-XDH retained on the DNA scaffold. Thus the volume analysis was conducted for the plausible XDH portion (next to the DNA scaffold in red square). (g) Frequency distribution of XDH volumes of sXDH (195 DNA scaffold assembled with HG-XDH analyzed). XDH exhibited frequency distributions covering a broad range of volumes corresponding to 2 dimers (30%), 3 dimers (55%) and 4 dimers (15%) of XDH, respectively. On average, 2.85 dimers of XDH were loaded on each DNA scaffold (2 × 15% + 3 × 55% + 4 × 15% = 2.85). Considering 88.4% DNA scaffolds were observed to bind with HG-XDH ($P_{HG\text{-}XDH}$ = 88.4%) (Table S2), the actual number of bound HG-XDH was calculated as followed. $N'_{HG\text{-}XDH}$ = 88.4% × 2.85 = 2.519 (molecules of HG-XDH dimer on each DNA scaffold) (Note S1), which was consistent well with the value (2.51) obtained by direct counting.

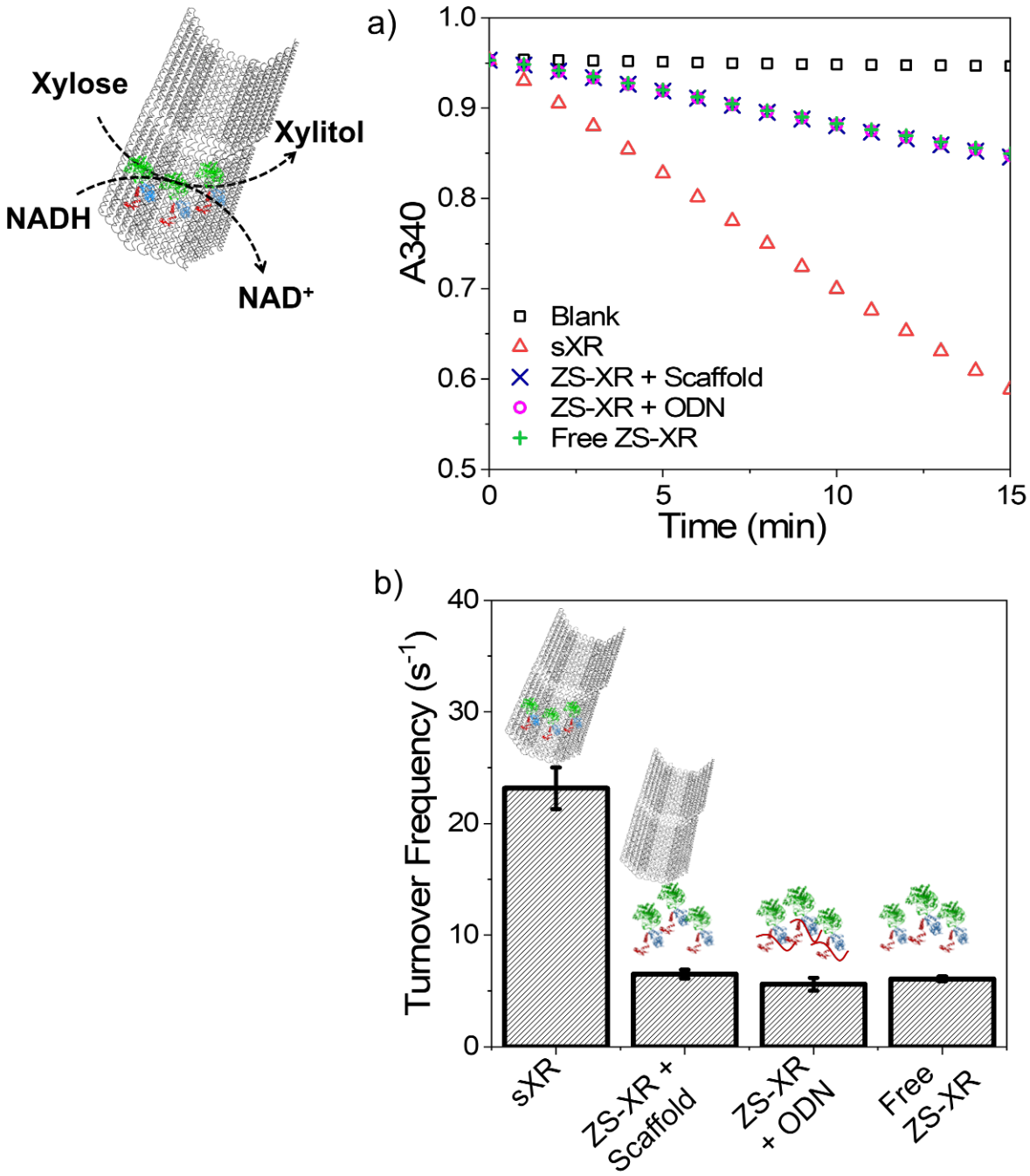

Figure S11. Catalytic activities of ZS-XR loaded on the DNA scaffold and free ZS-XR. (a) Time course of absorbance at 340 nm (A340) of enzyme reactions at the initial stage for scaffolded ZS-XR (sXR), free ZS-XR in the presence of DNA scaffold without its binding sites (ZS-XR + Scaffold), ZS-XR modified with a BG modified oligodeoxynucleotide (ZS-XR + ODN) and free ZS-XR in solution (Free ZS-XR). (b) Comparison of the turnover frequency of each enzyme reaction. Enzyme reactions were carried out by 5 nM (monomer) ZS-XR or sXR reacting with 200 mM xylose and 300 μM NADH in the buffer (pH 7.0) containing 40 mM Tris, 20 mM acetic acid, 12.5 mM $MgCl_2$, 5 μM BSA, 0.002% Tween20, 1 μM $ZnCl_2$ and 100 mM NaCl at 25 °C.

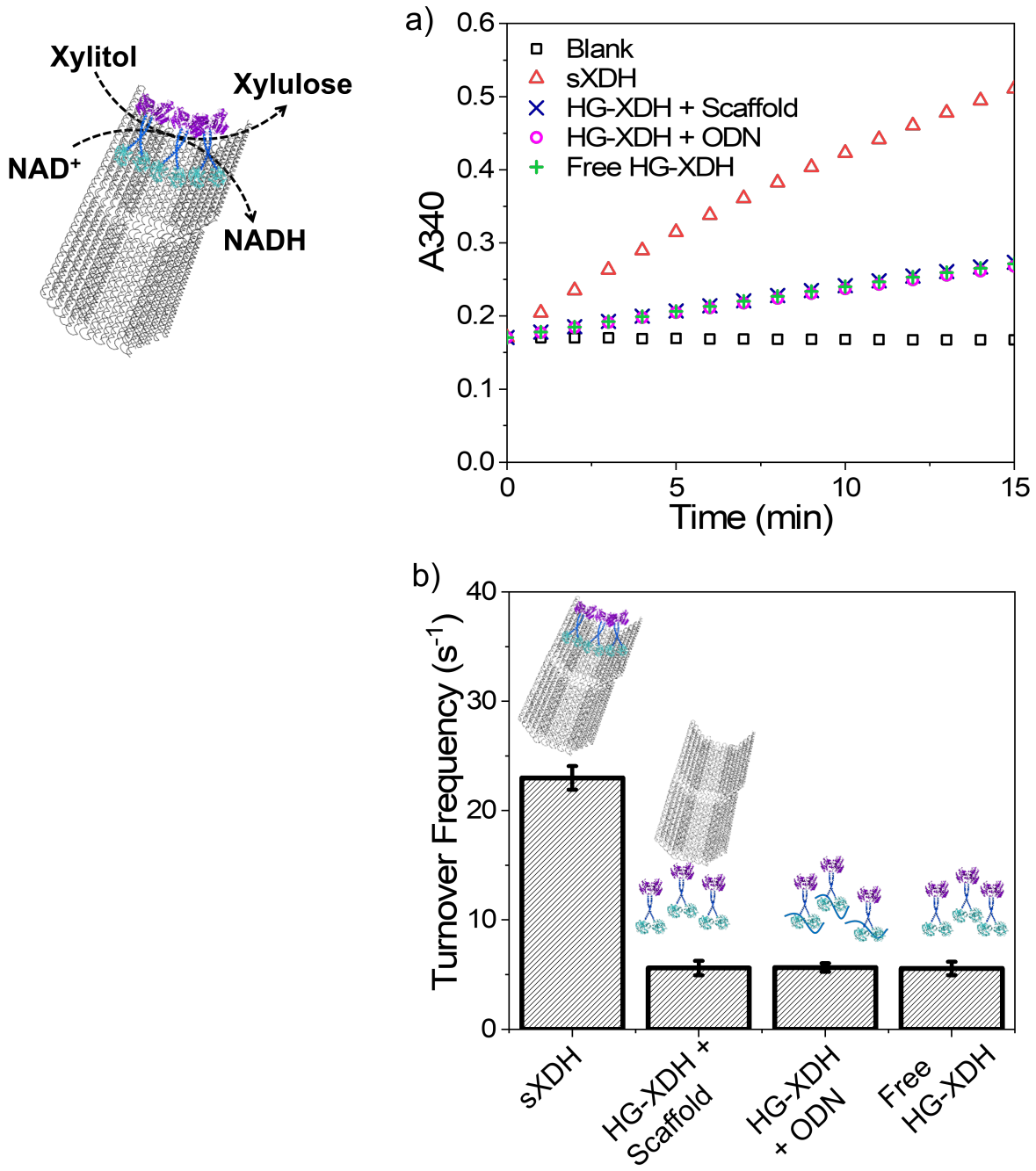

Figure S12. Catalytic activities of HG-XDH loaded on the DNA scaffold and free HG-XDH. (a) Time course of A340 of enzyme reactions at the initial stage for scaffolded HG-XDH (sXDH), free HG-XDH in the presence of DNA scaffold without its binding sites (HG-XDH + Scaffold), HG-XDH modified with a CH modified oligodeoxynucleotide (HG-XDH + ODN) and free HG-XDH in solution (Free HG-XDH). (b) Comparison of the turnover frequency of each enzyme reaction. Enzyme reactions were carried out by 5 nM (dimer) HG-XDH or sXDH reacting with 300 mM xylitol and 2 mM NAD^+ in the buffer (pH 7.0) containing 40 mM Tris, 20 mM acetic acid, 12.5 mM $MgCl_2$, 5 μM BSA, 0.002% Tween20, 1 μM $ZnCl_2$ and 100 mM NaCl at 25 °C.

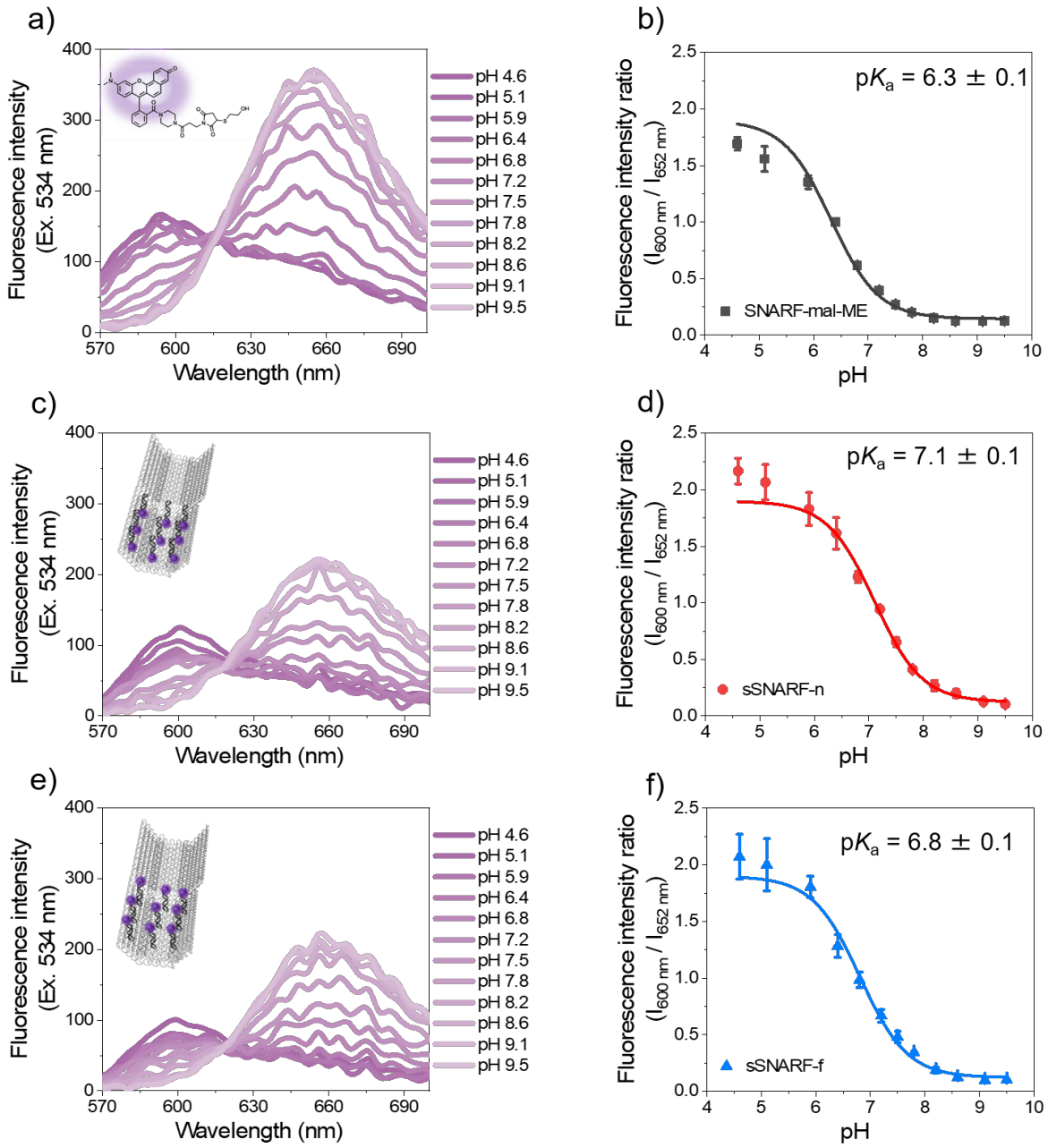

Figure S13. Titration of fluorescence emissions for SNARF-mal-ME, sSNARF-n and sSNARF-f by buffer pH. (a) Fluorescence emission spectra of SNARF-mal-ME in the buffer with different pH (4.6 to 9.5). (b) Plots of the emission ratio (I_{600} / I_{652}) against pH for SNARF-mal-ME. (c) Fluorescence emission spectra of sSNARF-n in the buffer with different pH (4.6 to 9.5). (d) Plots of the emission ratio (I_{600} / I_{652}) against pH for sSNARF-n. (e) Fluorescence emission spectra of sSNARF-f in the buffer with different pH (4.6 to 9.5). (f) Plots of the emission ratio (I_{600} / I_{652}) against pH for sSNARF-f. Fluorescence emission of 45 nM SNARF-mal-ME, sSNARF-n or sSNARF-f was monitored upon excitation at 534 nm in the buffer with different final pH (4.6 to 9.5) containing 0.002% Tween20 and 12.5 mM $MgCl_2$ at 25 °C.

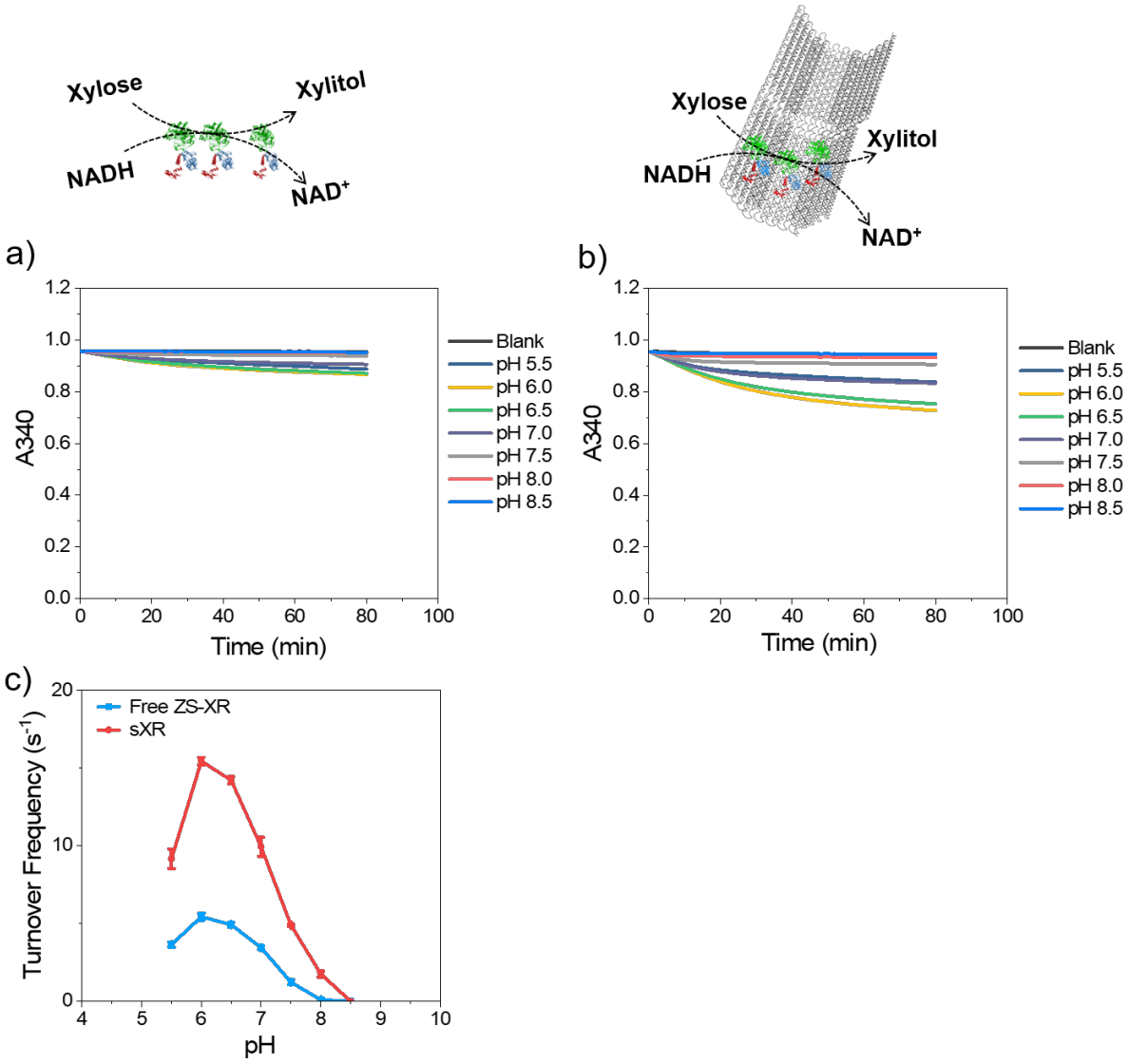

Figure S14. Reactions of free ZS-XR and scaffolded ZS-XR (sXR) at various buffer pH conditions. (a) Time course of A340 of free ZS-XR reaction in the buffer with different pH (5.5 to 8.5). (b) Time course of A340 of sXR reaction in the buffer with different pH (5.5 to 8.5). (c) Effect of pH on the turnover frequency of free ZS-XR and sXR reactions. Enzyme reactions were carried out by 2 nM (monomer) ZS-XR or sXR reacting with 200 mM xylose and 300 μM NADH in the Good's buffer with different pH (5.5 to 8.5) containing 12.5 mM $MgCl_2$, 5 μM BSA, 0.002% Tween20, 1 μM $ZnCl_2$ and 100 mM NaCl at 25 °C.

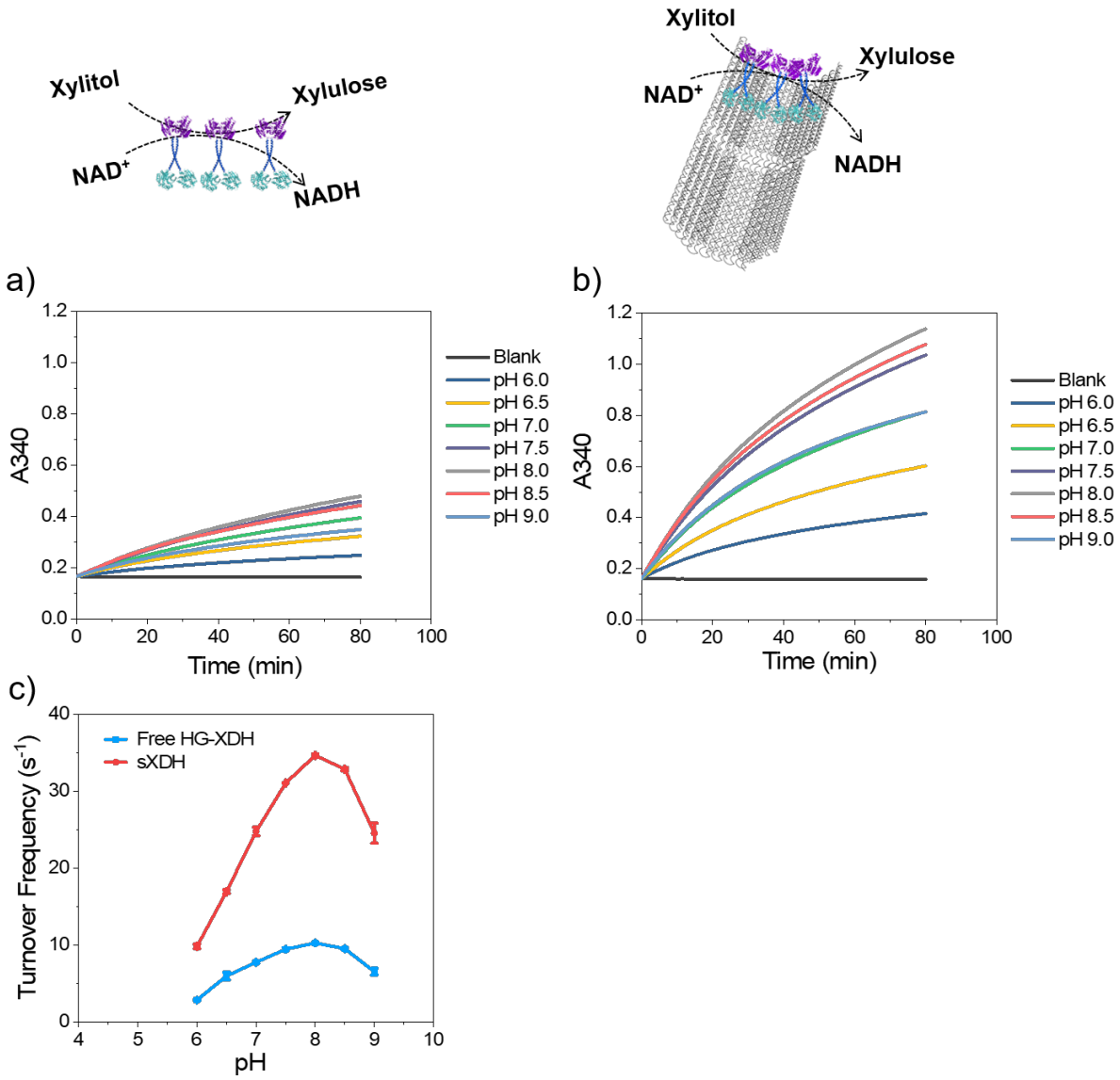

Figure S15. Reactions of free HG-XDH and scaffolded HG-XDH (sXDH) at various buffer pH conditions. (a) Time course of A340 of free HG-XDH reaction in the buffer with different pH (6.0 to 9.0). (b) Time course of A340 of sXDH reaction in the buffer with different pH (6.0 to 9.0). (c) Effect of pH on the turnover frequency of free HG-XDH and sXDH reactions. Enzyme reactions were carried out by 2.5 nM (dimer) HG-XDH or sXDH reacting with 300 mM xylitol and 2 mM NAD^+ in the Good's buffer with different pH (6.0 to 9.0) containing 12.5 mM $MgCl_2$, 5 μM BSA, 0.002% Tween20, 1 μM $ZnCl_2$ and 100 mM NaCl at 25 ℃.

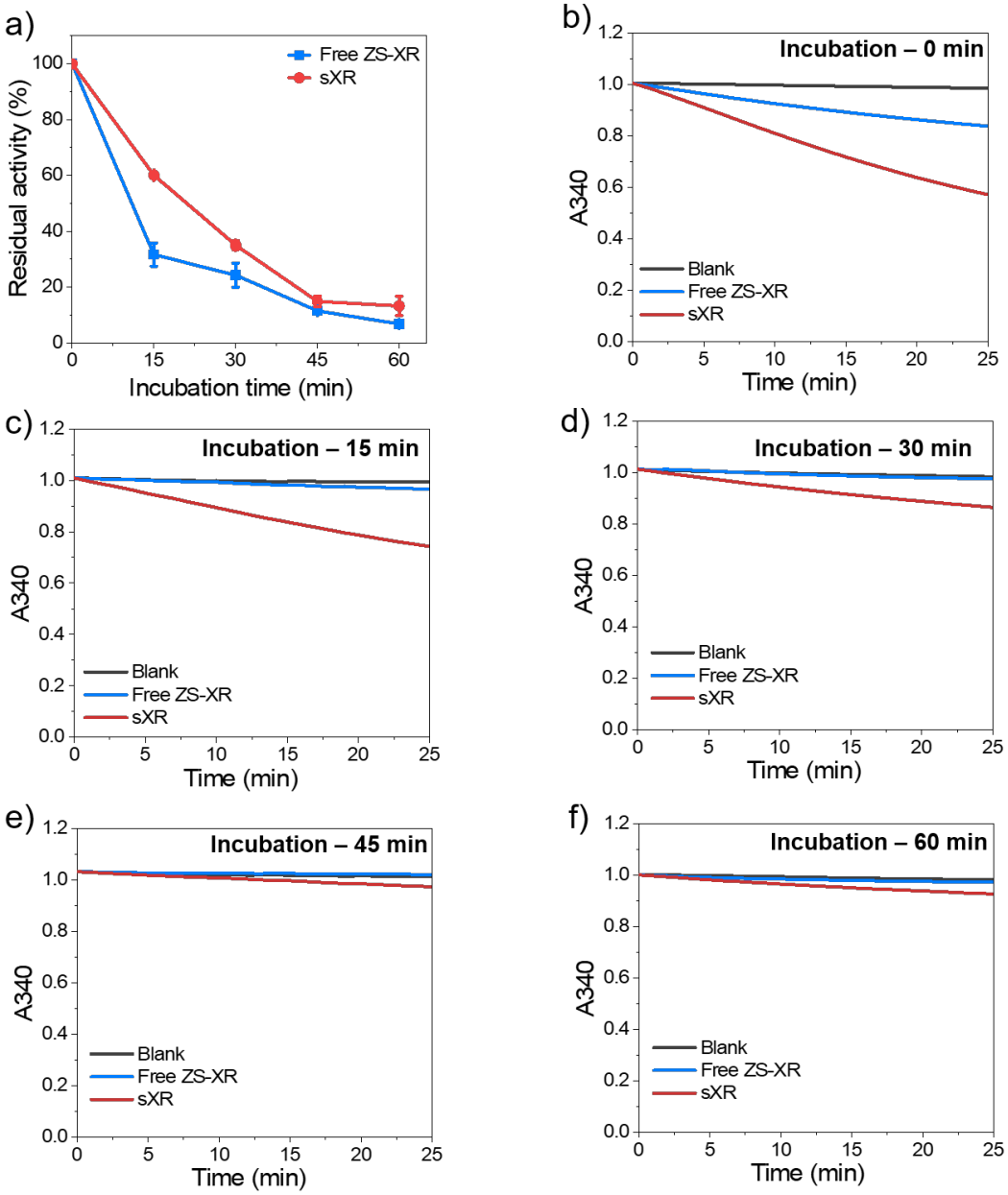

Figure S16. Residual activities of free ZS-XR and scaffolded ZS-XR (sXR) upon pre-incubation with BSA at ambient temperature. 6 nM (monomer) free ZS-XR or sXR was incubated with 5 μM BSA and 0.002% Tween20 in a buffer (pH 7.0) containing 40 mM Tris-HCl, 20 mM acetic acid and 12.5 mM $MgCl_2$ at 25 ℃ prior to the assay of catalytic activity. The enzyme activities were measured at the interval of 15 min with the final enzyme concentration of 2.5 nM. (a) Plots of the residual activity of enzyme against the pre-incubation time. The enzyme activities of free ZS-XR and sXR (incubation - 0 min) were set to 100%, respectively. Time course of A340 for enzyme reactions (b) without the pre-incubation, (c) after 15 min, (d) after 30 min, (e) after 45 min, and (f) after 60 min pre-incubation. Enzyme reactions were carried out by 2.5 nM (monomer) free ZS-XR or sXR reacting with 200 mM xylose and 300 μM NADH in the buffer (pH 7.0) containing 40 mM Tris, 20 mM acetic acid, 12.5 mM $MgCl_2$, 5 μM BSA, 0.002% Tween20, 1 μM $ZnCl_2$ and 100 mM NaCl at 25 ℃.

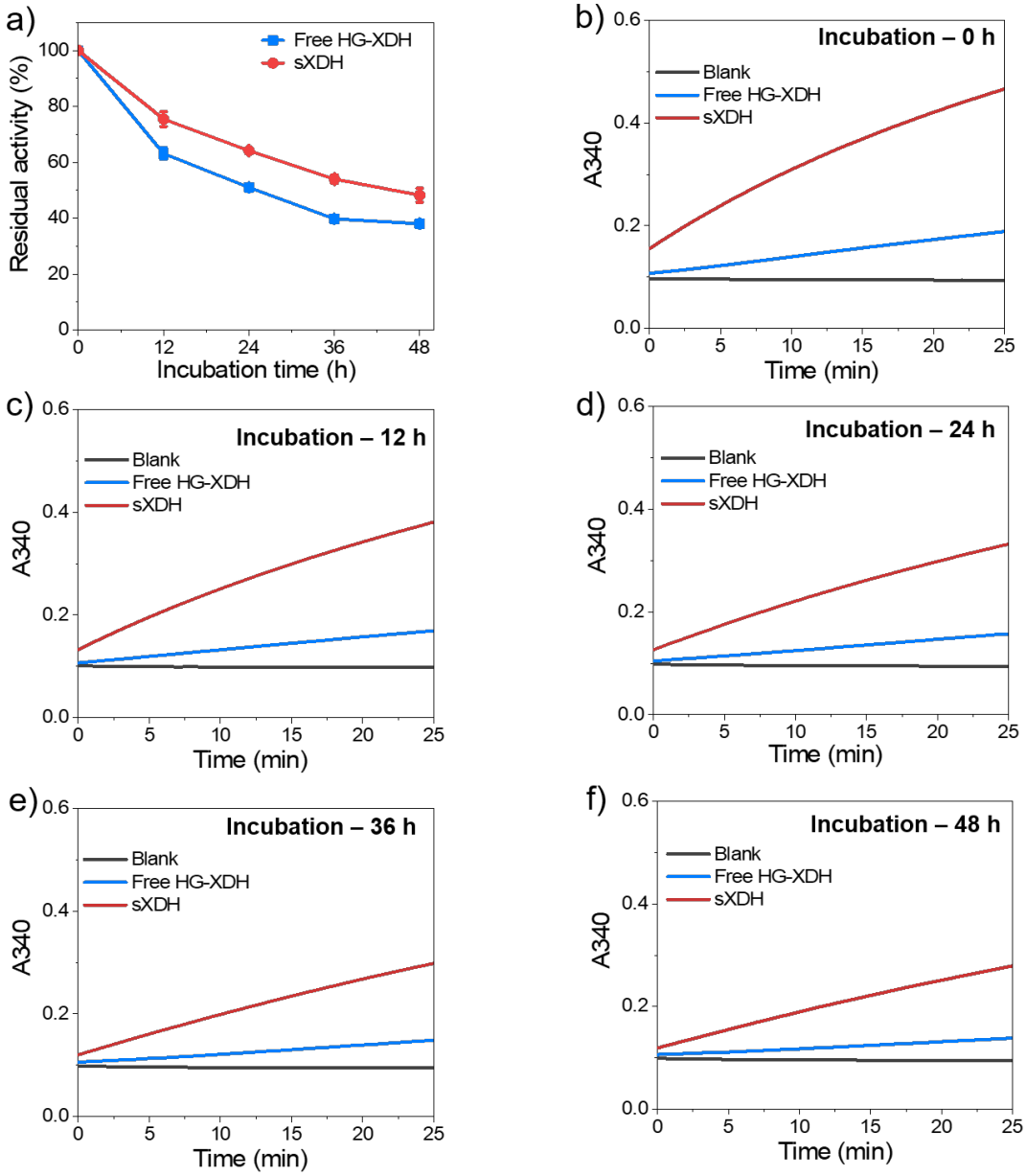

Figure S17. Residual activities of free HG-XDH and scaffolded HG-XDH (sXDH) upon pre-incubation with BSA at ambient temperature. 6 nM (dimer) free HG-XDH or sXDH was incubated with 5 μM BSA and 0.002% Tween20 in a buffer (pH 7.0) containing 40 mM Tris-HCl, 20 mM acetic acid and 12.5 mM $MgCl_2$ at 25 ℃ prior to the assay of catalytic activity. The enzyme activities were measured at the interval of 12 h with the final enzyme concentration of 2.5 nM (dimer). (a) Plots of the residual activity of enzyme reactions against the pre-incubation time. The enzyme activities of free HG-XDH and sXDH (incubation - 0 h) were set to 100%, respectively. Time course of A340 for enzyme reactions (b) without the pre-incubation, (c) after 12 h, (d) after 24 h, (e) after 36 h, and (f) after 48 h pre-incubation. Enzyme reactions were carried out by 2.5 nM (dimer) free HG-XDH or sXDH reacting with 300 mM xylitol and 2 mM NAD^+ in the buffer (pH 7.0) containing 40 mM Tris, 20 mM acetic acid, 12.5 mM $MgCl_2$, 5 μM BSA, 0.002% Tween20, 1 μM $ZnCl_2$ and 100 mM NaCl at 25 ℃.

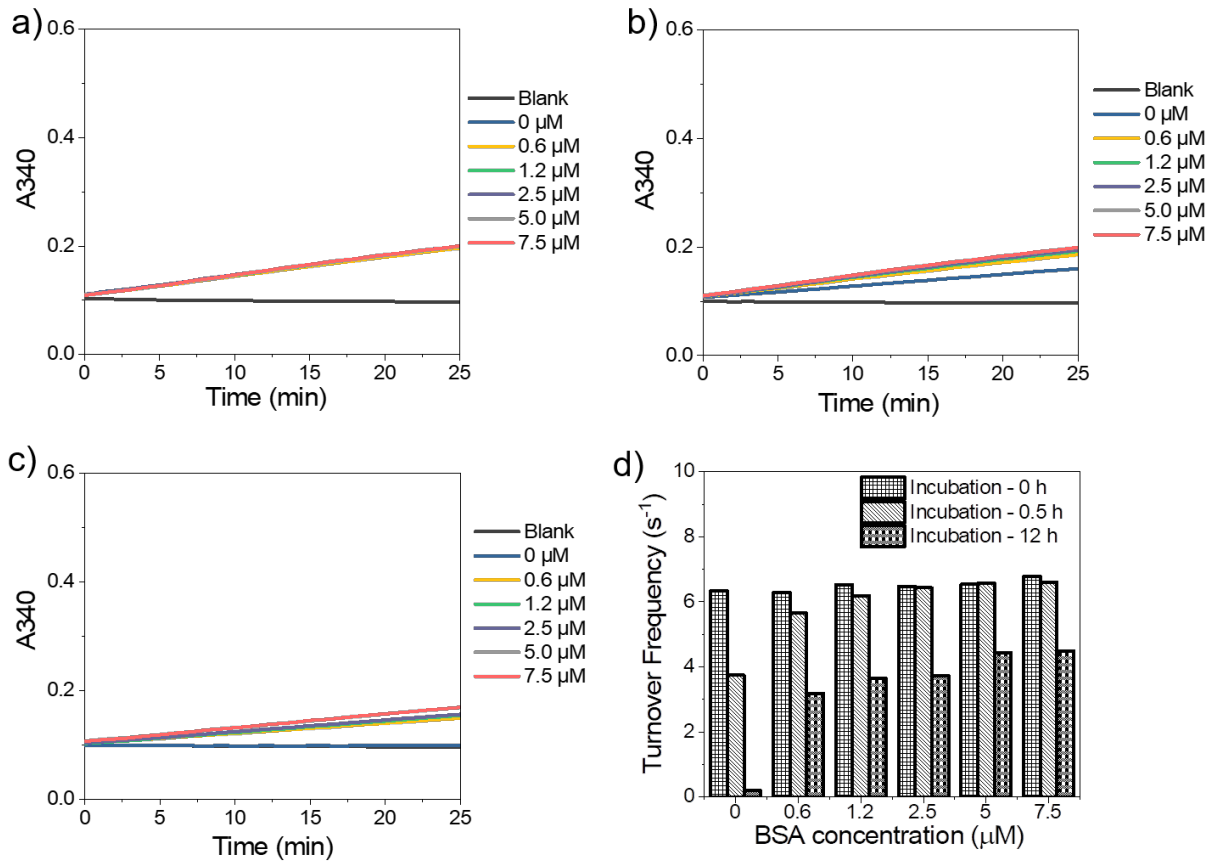

Figure S18. Concentration dependent effects of BSA on the residual activity of free HG-XDH against the pre-incubation time. Free HG-XDH (6 nM) was incubated with 0 to 7.5 μM BSA in a buffer (pH 7.0) containing 40 mM Tris-HCl, 20 mM acetic acid and 12.5 mM $MgCl_2$ at 25 ℃ prior to the assay of catalytic activity. (a) Time course of A340 for HG-XDH enzyme reactions without the pre-incubation. (b) Time course of A340 for HG-XDH enzyme reactions after 0.5 h pre-incubation. (c) Time course of A340 for HG-XDH enzyme reactions after 12 h pre-incubation. (d) Comparison of turnover frequencies of HG-XDH after pre-incubation for 0 h, 0.5 h and 12 h. Enzyme reactions were carried out by 2.5 nM free HG-XDH (dimer) reacting with 300 mM xylitol and 2 mM NAD^+ in the buffer (pH 7.0) containing 40 mM Tris, 20 mM acetic acid, 12.5 mM $MgCl_2$, 5 μM BSA, 0.002% Tween20, 1 μM $ZnCl_2$ and 100 mM NaCl at 25 ℃.

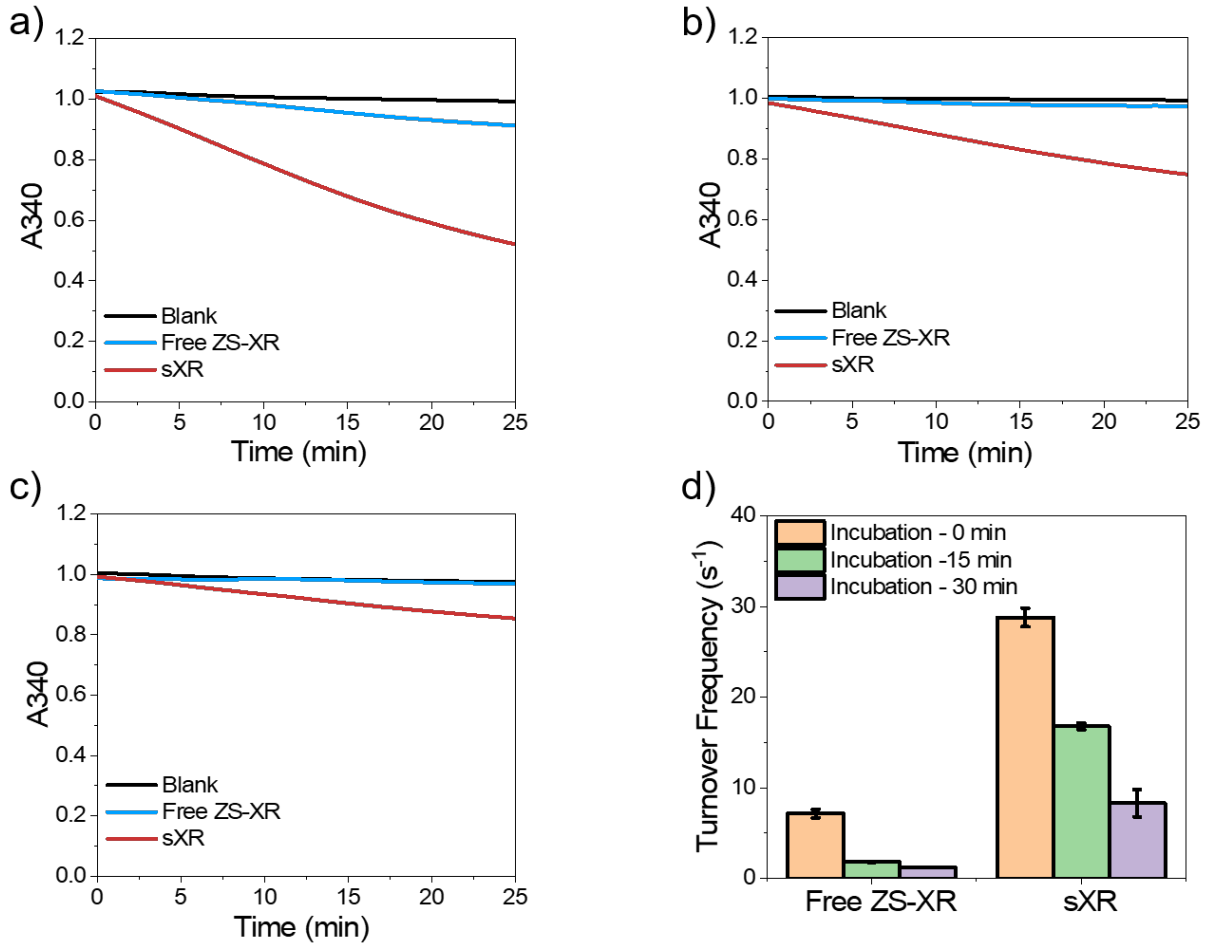

Figure S19. Residual activities of free ZS-XR and scaffolded ZS-XR (sXR) against the pre-incubation time without the addition of BSA. Free ZS-XR or sXR (6 nM) was incubated at 25 °C in a buffer (pH 7.0) containing 40 mM Tris-HCl, 20 mM acetic acid and 12.5 mM $MgCl_2$ prior to the assay of catalytic activity. (a) Time course of A340 for ZS-XR enzyme reactions without the pre-incubation. (b) Time course of A340 for ZS-XR enzyme reactions after 15 min pre-incubation. (c) Time course of A340 for ZS-XR enzyme reactions after 30 min pre-incubation. (d) Comparison of turnover frequencies of free ZS-XR and sXR after pre-incubation for 0 min, 15 min and 30 min. Enzyme reactions were carried out by 2.5 nM (monomer) free ZS-XR or sXR reacting with 200 mM xylose and 300 μM NADH in the buffer (pH 7.0) containing 40 mM Tris, 20 mM acetic acid, 12.5 mM $MgCl_2$, 5 μM BSA, 0.002% Tween20, 1 μM $ZnCl_2$ and 100 mM NaCl at 25 °C.

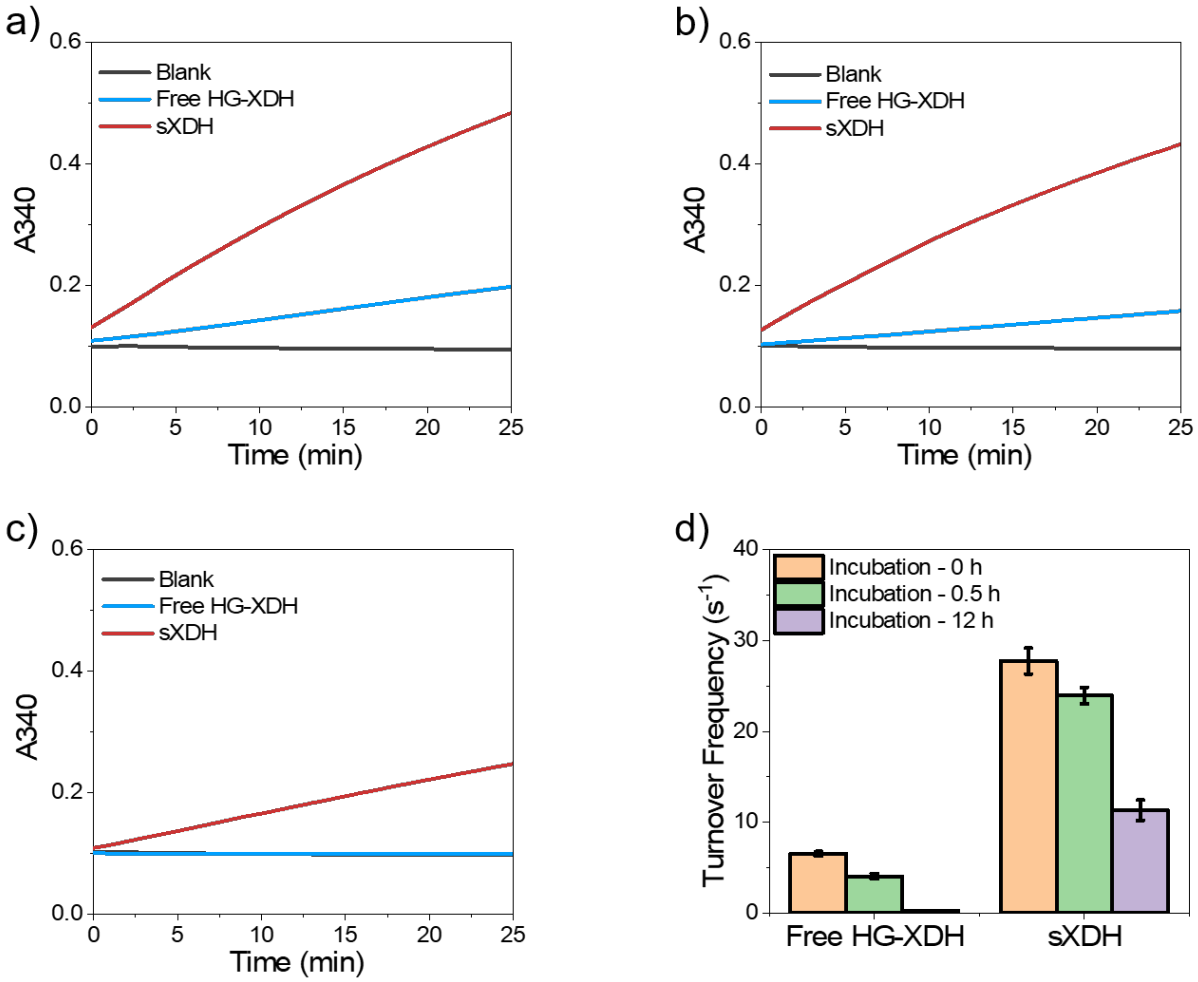

Figure S20. Residual activities of free HG-XDH and scaffolded HG-XDH (sXDH) against the pre-incubation time without the addition of BSA. Free HG-XDH or sXDH (6 nM) was incubated at 25 ℃ in a buffer (pH 7.0) containing 40 mM Tris-HCl, 20 mM acetic acid and 12.5 mM $MgCl_2$ prior to the assay of catalytic activity. (a) Time course of A340 for HG-XDH enzyme reactions without the pre-incubation. (b) Time course of A340 for HG-XDH enzyme reactions after 0.5 h pre-incubation. (c) Time course of A340 for HG-XDH enzyme reactions after 12 h pre-incubation. (d) Comparison of turnover frequencies of free HG-XDH and sXDH after pre-incubation for 0 h, 0.5 h and 12 h. Enzyme reactions were carried out by 2.5 nM (dimer) free HG-XDH or sXDH reacting with 300 mM xylitol and 2 mM NAD^+ in the buffer (pH 7.0) containing 40 mM Tris, 20 mM acetic acid, 12.5 mM $MgCl_2$, 5 μM BSA, 0.002% Tween20, 1 μM $ZnCl_2$ and 100 mM NaCl at 25 ℃.

Figure S21. Agarose gel electrophoretic analysis of the DNA scaffold before and after the purification. The gel was stained with ethidium bromide (EtBr) and visualized by using Molecular Imager FX pro (Biorad). Lane M: 1 kb DNA marker, Lane 1: DNA scaffold (20 nM before purification). Lane 2: DNA scaffold after purification by size exclusion chromatography using 500 µL volume of Sephacyl S-400 in Ultrafree-MC-DV column. Gel electrophoresis conditions: 1% agarose in 1 × TAE buffer with 12.5 mM $MgCl_2$, 50 V, 2 h.

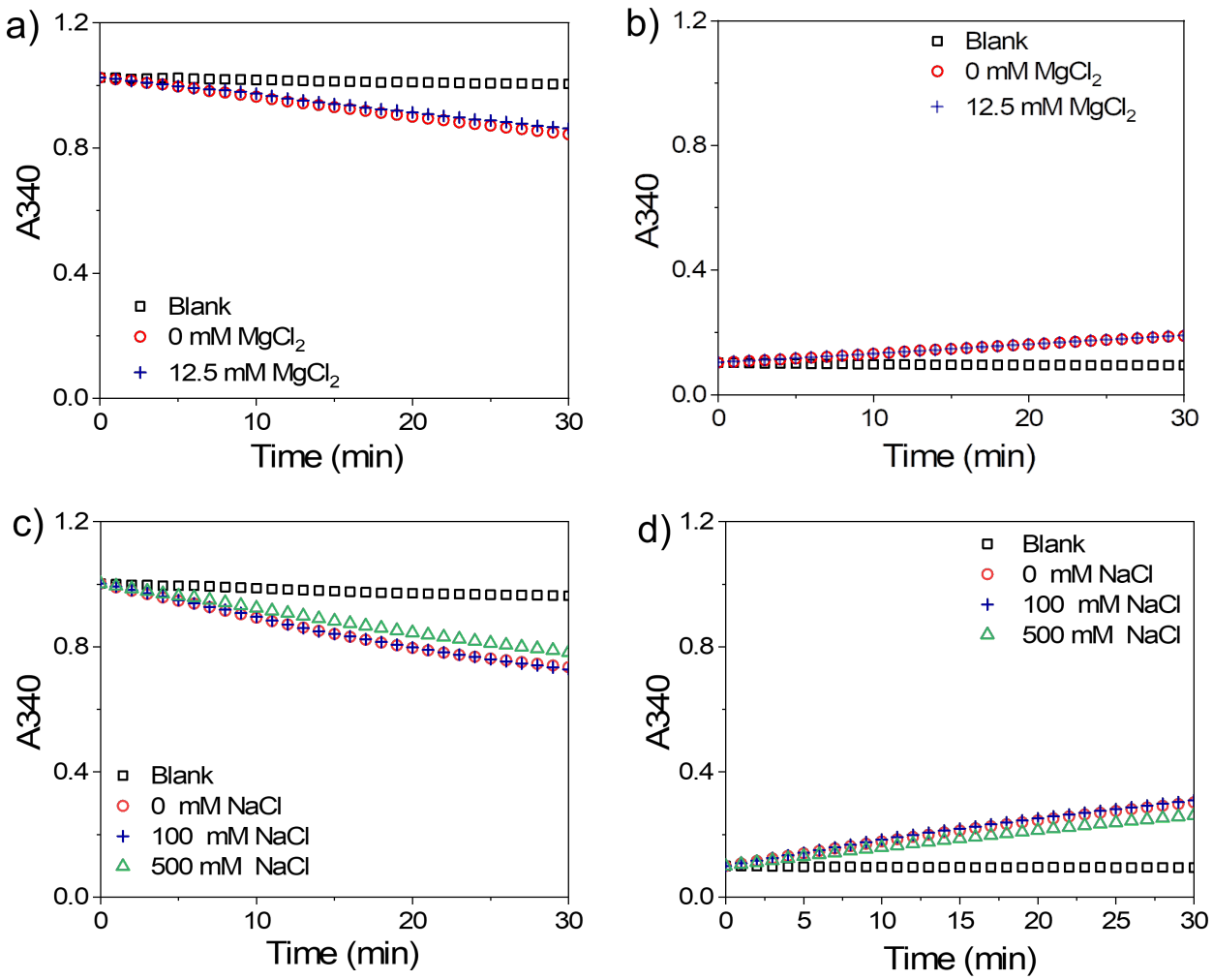

Figure S22. The effect of $MgCl_2$ and NaCl on the enzyme activity of free enzymes. (a) Time course of A340 of free ZS-XR reaction in the absence or presence of 12.5 mM $MgCl_2$. Enzyme reactions were carried out by 2.5 nM (monomer) free ZS-XR reacting with 200 mM xylose and 300 μM NADH in the buffer (pH 7.0) containing 40 mM Tris-HCl, 5 μM BSA, 0.002% Tween20, 1 μM $ZnCl_2$ and 100 mM NaCl at 25 °C. (b) Time course of A340 of free HG-XDH reaction in the absence or prescence of 12.5 mM $MgCl_2$. Enzyme reactions were carried out by 2.5 nM (dimer) free HG-XDH reacting with 300 mM xylitol and 2 mM NAD^+ in the buffer (pH 7.0) containing 40 mM Tris-HCl, 5 μM BSA, 0.002% Tween20, 1 μM $ZnCl_2$ and 100 mM NaCl at 25 °C. (c) Time course of A340 of free ZS-XR reaction in the absence or presence of NaCl. Enzyme reactions were carried out by 5 nM free ZS-XR reacting with 200 mM xylose and 300 μM NADH in the buffer (pH 7.0) containing 40 mM Tris, 20 mM acetic acid, 12.5 mM $MgCl_2$, 5 μM BSA, 0.002% Tween20, and 1 μM $ZnCl_2$ at 25 °C. (d) Time course of A340 of free HG-XDH reaction in the absence or presence of NaCl. Enzyme reactions were carried out by 5 nM (dimer) free HG-XDH reacting with 300 mM xylitol and 2 mM NAD^+ in the buffer (pH 7.0) containing 40 mM Tris, 20 mM acetic acid, 12.5 mM $MgCl_2$, 5 μM BSA, 0.002% Tween20, and 1 μM $ZnCl_2$ at 25 °C.

Table S1. Nucleotide sequences for the staple strands containing the binding sites for ZS-XR with BG modification or the binding sites for HG-XDH with CH modification

Oligo DNA	**Sequence (from 5' to 3')**
Binding site 1	GGGGGATCAGCCAGCTTACGCCCACGCGCGTT^{BG}TTCGCGCGTGGG CGTAAGCTTTCCGCAAACGG
Binding site 2	GGAAGCCGGAAGCACTTACGCCCACGCGCGTT^{BG}TTCGCGCGTGGG CGTAAGAACTCCAGTTGATT
Binding site 3	GCATAACAAATCTCCTTACGCCCACGCGCGTT^{BG}TTCGCGCGTGGG CGTAAGCAAAAAATTTCTGT
Binding site 4	TACCAGATTAAGACGT^{CH}TCATGAGTCATGAGTTTTCT^{CH}CATGACT CATGAACTCCTTATCGATTGA
Binding site 5	TGTAAATGATAGCTGT^{CH}TCATGAGTCATGAGTTTTCT^{CH}CATGACT CATGAACTAGATTATTAATTA
Binding site 6	ATAACATGCAACAGGT^{CH}TCATGAGTCATGAGTTTTCT^{CH}CATGACT CATGAACGAAAAACGTAAGAA

BG modified amino-C6-T was denoted as $\mathbf{T^{BG}}$

CH modified amino-C6-T was denoted as $\mathbf{T^{CH}}$

Table S2. Average number of assembled enzyme

Scaffolded enzyme	**Modular adaptor enzymes**	**Number of well-formed DNA scaffold**	**Numbers of enzymes on modified sites [yield]**				**Average number of assembled enzyme**
			Three-binding	**Two-binding**	**One-binding**	**Empty**	
sXR	ZS-XR	253	187 [73.9%]	28 [11.1%]	26 [10.3%]	12 [4.7%]	2.54[1]
sXDH	HG-XDH	376	295 [78.4%]	22 [5.8%]	16 [4.2%]	43 [11.4%]	2.51[2]

Note:

[1] Calculation of average assembly yield of ZS-XR on DNA scaffold

$N_{ZS\text{-}XR} = 3 \times 73.9\% + 2 \times 11.1\% + 1 \times 10.3\% + 0 \times 4.7\% = 2.54$ (molecules of ZS-XR monomer on each DNA scaffold)

[2] Calculation of average assembly yield of HG-XDH on DNA scaffold

$N_{HG\text{-}XDH} = 3 \times 78.4\% + 2 \times 5.8\% + 1 \times 4.2\% + 0 \times 11.4\% = 2.51$ (molecules of HG-XDH dimer on each DNA scaffold)

Table S3. Nucleotide sequence for the thiol modified ODN

Oligo DNA	**Sequence (from 5' to 3')**
ODN-thiol	**Thiol -** GGATTCGGCTCTTCAGCGAA

Table S4. Nucleotide sequences used for the hybridization with SNARF modified ODN

Oligo DNA	**Sequence (from 5' to 3')**
3SR-37-out1	GAAGCCCTACATACTTCGCTGAAGAGCCGAATCCTAATAATAA
3SR-36-in1	TTCGCTGAAGAGCCGAATCCATAAAGGATATGGT
4SR-37-out2	AAGCAGATATGTTATTCGCTGAAGAGCCGAATCCTAATAATAA
4SR-36-in2	TTCGCTGAAGAGCCGAATCCGCAAACGGACAAAA
5SR-37-out3	TACCAGATTAAGACTTCGCTGAAGAGCCGAATCCTAATAATAA
5SR-36-in3	TTCGCTGAAGAGCCGAATCCTCCTTATCGATTGA
3WX-46-out4	AATCGCATAGAATCTTCGCTGAAGAGCCGAATCCTAATAATAA
3WX-47-in4	TTCGCTGAAGAGCCGAATCCCTTGAAAATTTGAA
4WX-46-out5	TGTAAATGATAGCTTTCGCTGAAGAGCCGAATCCTAATAATAA
4WX-47-in5	TTCGCTGAAGAGCCGAATCCTAGATTATTAATTA
6WX-46-out6	AGGTTGGGAGAAGATTCGCTGAAGAGCCGAATCCTAATAATAA
6WX-47-in6	TTCGCTGAAGAGCCGAATCCGTCAATAACAAACA
3cb-57-out7	TCACGCATCAATCGTTCGCTGAAGAGCCGAATCCTAATAATAA
3cb-56-in7	TTCGCTGAAGAGCCGAATCCTCTGAAAACATTCT
4cb-57-out8	GCAATACGAAATACTTCGCTGAAGAGCCGAATCCTAATAATAA
4cb-56-in8	TTCGCTGAAGAGCCGAATCCCTACATTGAACCCT
5cb-57-out9	ATAACATGCAACAGTTCGCTGAAGAGCCGAATCCTAATAATAA
5cb-56-in9	TTCGCTGAAGAGCCGAATCCGAAAAACGTAAGAA

Table S5. Unmodified staple strands used for the assembly of the DNA origami scaffold

Oligo DNA	**Sequence (from 5' to 3')**
1	AAAATCCCTTATAATGCCAGCTGCATTACTCACTG
2	GATGGTGGTTCCGAGGCCAACGCGCGGGACTCACA
3	CAGCAGGCGAAAATGGTTTGCGTATTGGGGGTGCC
4	GAGAGTTTGAGACGGGCAACATCCACACAACATACGCTGTTT
5	TTTCTTTAAGCATAAAGTGTAGAATTCGTAATCATCTCTTCG
6	CCCGCTTACGGCCAGTGCCAAGCCAGGGTTTTCCCTGAGGGG
7	TTAATTGTGCCTGCAGGTCGAAAGGCGA
8	TAATGAGGGATCCCCGGGTACGGCGAAA
9	CTCAAGCCTGGCGCCAGTTTGCCC
10	ATAGAGCCGGTCACCAGGCAGCAA
11	CCTGTGTGGAAGGGCGATCGGAAAGCGC
12	TTAAGTTGGCCTCAGGAAGATTGGGATA
13	GGGGGATCAGCCAGCTTTCCGCAAACGG
14	CTATTACTTCTGGTGCCGGAACCGTCGG
15	ACGACGAAGATGGGCGCATCGGTTCTAGGATGAACGGTAA
16	CATTCGCTAAATGTGAGCGAGGCGTCTGATTCGCATTGTAAA
17	GGTCACGCCGGAGATCTGGAGGTACCCC
18	CGGATTGGAGAGATCTACAAAGTAATGT
19	ATTCTCCGAACGCCAATCAGCTTGTATA
20	GAGAATCCTGATAAGACAGTCAAATCACGGCAAAGAACA
21	CTGAGAGGGGTAGCAAAAGGGTGAGAAAAGCA
22	TATCAGGAAAGCCCCAAAAACGGGCGCGAATCGGTTGTACCATGCC
23	TGTTAAAGCCTTCCAAAATTTTTAGAACACTT
24	TCGTAAAACTAGCATGTCATAGCATTAATTAGCAAAATTAGGCC
25	GGTTGATCATCAATAAGCCTCAGAGCATAAG
26	AGCAAATGTTTAGCTATGACCCTGTAATCCT

27	CGTTAATTTCGCAACGGGAGA
28	GGAATTAATGTTGGTGTCAGTATCGGGTAACGCTTGCACGTTGCG
29	ATTCTATTTTTACCGTAACGCACTCGTGCTGCCTCTAGATGAGCTA
30	GTAGGTAAAAGCTAAGCTGAAGTGTCTGCCTTTAACAGA
31	TGACCAATAGGTGGGAAGCACCGCGCCAGCTCGAG
32	AATGCAAAAAACATTATATTTTATAACAACAGGTCCAAA
33	CATAATAATTCTAACAACACCAGGCTGCGGGCGGTC
34	ATATCTACTATAAATATAAGAGGTCTTT
35	TTGATGGTCACTGCGAACCAGACCCGAA
36	TCCATGCTGTGCTTAGAACCATAATTAA
37	CATGTTTATAGTAGATCATATCAAACAA
38	AAGTACGAAGGTGGAATCAGATCATTGC
39	CATTCCATCATTTGAGGAAGATCATTTTTTAAGGC
40	CCCAATTATAACCTATTTAAATTAAATTTTTGTTAATCAAAATATTTTA
41	AGCTTCAAAGCGAACGAGTAGATTTAGT
42	ATCAGGTCATTTTTGCGGATGAGCTCAA
43	ACCATTGAATAAGGAATGGTAGAAGACG
44	TTATAGTTTGCTCCTTTTGATGCAACTA
45	AGCGCGGAATAGAGCAATAACGGATAGT
46	ATTGCATAGGATTAGAGAGTAGAAGTTT
47	AAGGACTGGATCGTTTAATCTACGGTTT
48	GGAAGCCGGAAGCAAACTCCAGTTGATT
49	AGAGGGGTAAAAACCAAGTCAGGATTGTGAAAGATGAA
50	ACAAATGCAGAGATTTATCAGTGAAAATCAA
51	AAGTTTTGCCAGAGCTTCAAATATCGCG
52	ACGCCAACCCCCTCAAATGCTATCAAAA
53	CATAGTACGTCATAAATATTCCTGACTA
54	ATAACCCTAGCGTCCAATACTAAAGCGG

55	ACGATAATAGTAAAATGTTTAATTAAGA
56	AGAAGAACCGGATATTCAGCGAAAACTTTTT
57	AAATCATCAAGAGTAATGAGGGTACAGAGGC
58	AATGGCGCATAGGCTGGGAACGAGCGACCTG
59	CCCATAAGGCTTGCCCTAGATTCAGAAGGCA
60	ACAAACACCAGAACGAGACAACATAAGAGGC
61	CCTTTGGGCTTGAGATGTTAATAAAAACACT
62	CCATTCAACTTTAATCACGTTGGGAGCGATT
63	CGGTGTATCATAAGGATAAAT
64	TTGAAAGAGGACTTACCTTATGCGATTTTAA
65	CATGAGGCCACTACTCAGTTGATACATA
66	TTTGAGGAAAACGATATTACATACGAGG
67	CTCCATGTACACTAAACGAACCACTATC
68	TGTGTCGGACCCCCAAGAAAACCAGACG
69	TTGTATCGCGCGAATATACCAAATAGCG
70	CGTAATGAAGTTTCTCGTCACGGAGTTA
71	CCAACCTACTAAAGGACAGCATTCGGTC
72	AAAAGAATTGGCTAGCAACACCGCCCAC
73	CATCTTTAAATCCGGCGCAGAGCCGACA
74	ATACCAAATCGCCTGGAACCGCAGCTTGATACCGATCGGTTT
75	GCTGAGGATAATAATTTTTTCAACAACT
76	GCATAACAAATCTCCAAAAAATTTCTGT
77	ATGACAACAAAAGGAGCCTTTTCCAGAC
78	GAATTTCTTAAAAACTGACCAACT
79	TAAAGGACGGAGTGAGAATAGACCCTCATTTTCAGGCCACCC
80	ATCAGCTGATCTAAAGTTTTGTGTAGCA
81	CAGATTGCGACTTGCAGCCTCAGCATTA
82	TTCAACAAAGCCCAATAGGAAAGAACCGCCACCCTTGAAACATGAAAGT

83	CTAACGTTGACGATATATCGGAACCTTG
84	ATGGGATACCGTAACACTGAGAGGTTTAGTACCGCGGCTGAG
85	GAATAAGGCTCCAACCATTTAGCCGCTGA
86	GTTAGTAACCAGTACAAACTAAGGTGTATCACCGTGGATTAGGATTAGC
87	TTCCACAGATATAAGTATAGC
88	CCGGAATCAACGCCTCGTCTTAATTGTATAGTTGCCGGTCAACAGA
89	ATTATTCCAGAACCGGATAGCGTTT
90	ATTAAGACACCCTCCCCATGTTTTG
91	AAGAGAAACTCAGGTTTCGTCAAT
92	ACAGGAGTGTACTGAATCCTCCTCCCTCCGGC
93	TGGCTTTGGAAAGCCAGAGCCCCTTATTCGTC
94	AGCCAGAACCCACCGTACAATGAATTATTTTCAAAGACGCAA
95	CAGCACCACCAATCAAGTAGCAAGAAAATTCTGGC
96	ATACAGAACCCAGACTGCACC
97	CCGCCACATTGACAGGAGGTTCGTATAA
98	TCAGAGCGTCAGACGATTGGCAGTGCCT
99	CCACCCTTTCACAAACAAATAGTAATAA
100	AAAATCACCGGAACGCAGTCTCTGAATT
101	ATTGGGAATTATTCAACTACGCAGTAGCCGAACAC
102	ATAGCCCACCACCGGAACCGCATTAAAG
103	AGTCGCCAAATAGAAAATTTTTAAGGTAATTTCCA
104	ACCAAGGTAAGGCATGAAGGAAACTTAGACGATAG
105	AGGTGAATTATCACAGCGTTTGCCATCT
106	TCAATAGGCCGGAAACGTCACATCAGTAGCGACAGCTCAGAG
107	TTACCAGAGCACCATTACCATTTTGCCTTTAGCGTGCCACCC
108	GGGCGACAGAGCCAGCAAAATTAGCGCGTTTTCATAGAGCCG
109	GGGAGGGGACTTGAGCCATTTTTCGGTC
110	AACATAGCTAGAGAGATCAGCCATCCTGAAT

111	AAGAACTATATTGACGGAAAT
112	GAAGAGTTAAATTTGCCCGAGCGT
113	AATAGCAATATAAAAGAAACGGTCACAA
114	GAAGCCCTACATACATAAAGGATATGGT
115	AAGCAGATATGTTAGCAAACGGACAAAA
116	TACCAGATTAAGACTCCTTATCGATTGA
117	CCTTGTTTAAAATCAAGATTAGTTTTCAATA
118	AATTGCACCCAGCTACAACGACGACGCCTGT
119	GATTTTTGAACAAACTTTCCTTATCATTCATTACC
120	AATGAAAGGAGAATCGGGTATTAAACCATTTT
121	CAGGCGGGAGGTTTTGATATAGAATTCATCG
122	TAAAGTTACAAAATAAAAACCCACCCTAATT
123	CTTACCAAGGTAAATAAGTCCTGAACAA
124	TATATTATTTATCCCAAGAGCGCTAACCAAT
125	GAACCTCTCTAAGAAACAAGCAAGCCGTAGTACCGAAGCGCACGAGGAA
126	GCAAGCAGGGCTTAATTGAGAAAATAAGAATAAACAACTATA
127	TTATCAAATGTAGAAATATCATCTTACC
128	GCGCCCAGCTAATGCGGCTGTGTCAGAGGAAAAGT
129	TAGGAATCCAAGAATAACTGAACAAAGT
130	ATTGGCTTATTAAAGCCAACGCTCTCATAATTACTAGACCGGCTT
131	ATAATATCCCATAAGAATTACAATGA
132	TACGAGCCAATAGAGTAATTCAATTTAG
133	CAATAATCAGAACGCAATAAATATTTAA
134	GCAGAGGTTTAATGGTTTGAAGAACGCG
135	CAACGCCCCGTGTGATAAATACAAATCC
136	GCCACAACATGGCTATTTAAGAAAC
137	TTATACAAATTCTTTGTTTAG
138	GAAAACAGTAAATCAGAAGCCTTACGTCAAA

139	GCCACCAGTACCGGTATCCGACTTCCTTTAC
140	AGAAAACCGCTATTAATTAATGGAAACA
141	AATCGCATAGAATCCTTGAAAATTTGAA
142	TGTAAATGATAGCTTAGATTATTAATTA
143	AGGTTGGGAGAAGAGTCAATAACAAACA
144	CGTTTTTTCAACCTAAACATTTTCCGACAAAACGC
145	CCTAGACAAAATACCGAAACATGTTGTCCAGATTT
146	GTACATATTGAGTATGGCAATCTTCTGA
147	TTACCTTCGGAACAATATTCCAGAACCT
148	CATTTAAAGTTGCTCCTGAGAATTTGCA
149	TCAAGAAACAAAATGGAGAAAAAAGAAA
150	AAGAAGATTATTCAGTAACAGAGGTTTA
151	AGACAATTTCACATAGCGCTGATGAGGCGTTATC
152	TCGTTGAATAATAGATAATACATTATCAATACCAG
153	TACATCGCGCGCAGACTAATAGATTAGAAAATCAATTAA
154	GATTGTTTGGCCACGCTGAGA
155	ATAATGGATTAACACATCACCTTGCTGACTTT
156	ACCATATAACAGAGATATCAAACCCTCATGAGGATCACC
157	CGTAAAACGAACCATCTGGTCAGTTGGCGCCG
158	TTGCGTAATCGCCACAGTTGAAAGGAATACTA
159	CGACAACTCTAAAGCCGCCTGAAAAGGGTGGA
160	ACACATTTTGTTTTAATTTTC
161	TATTAGAACCTCAAGTGAGGCAGAGATATTGA
162	TCACCAAGTTAACAAAAAGACGCTGTTATATACCG
163	ACAAGGCGAATGATGAAGTGAATTTTAACCTAAAA
164	TAGGAGCTGAGGAAGATAGCCGCTATTAATCC
165	TGAAAAATCGTATTTAAAAGTAATCAATAAAT
166	CAGTGAAAGCGCTCATGTTCTTTGACAG

167	AAACACAGACAGCCATTCACTTGCTAGAATCTTAATGC
168	CAGTAATCAACAGTGATTATATCATCAATATAATCTTAATTTAAATCCT
169	GGCCAACGGTCAGTAAGGGTTTGATTATCAGATGAACATTATAACAAT T
170	TCTGACCAAGATAACAAAATTGCGGAATTATCATCAAGAAACTTAGAA G
171	TACGTGGTACCGAACAGAAATCAATAACGGAT
172	TTGAATGCTAAAACGATTTTCTACCTTT
173	TTAAAAGAGTCAGAATCCGGGCGCAGCCGGCGTTGTTC
174	CGCAATTAACTTTTAGAGTGTAGCGATTTAGAGTCCAC
175	AGATCAAACTCGTATAACGTACTA
176	GGCCACCGAGTATTTACATTGGCA
177	TCACGCATCAATCGTCTGAAAACATTCT
178	GCAATACGAAATACCTACATTGAACCCT
179	ATAACATGCAACAGGAAAAACGTAAGAA
180	GAAGAACACAATATTACCGCCAATATTT
181	GAGTAACCACGGAACCCGACTCCA
182	GAAAGCGAAAGGAGCTGAGAA
183	GCCGCGCAGAGCGGGAGCTAAATTAGTA
184	CAGGGCGCGTGCTTTCCTCGTCTGAGTA
185	CGGGGAATAGGGCGCTGGCAACAGGAACGGTACGCCTGTCCA
186	AGCCCCCGGTCACGCTGCGCGGCCGATTAAAGGGACGTTGTA
187	AGATAGGGTTGAGTGAACGTG
188	ACGTCAAAGGGCGATAAAGCACTAAATCCACACCC
189	TCTATCAGGGCGATTTTTTTGGGGTCGAGCCGCTA
190	TGAGTAACAGTGCCGAGG

Table S6. Nucleotide sequences of connecting hinges to stabilize the fully open state of DNA scaffold

Oligo DNA	**Sequence (from 5' to 3')**
Connecting hinge 1	ACATTGAATATATTTTAGTTTTTTACGAGAATG
Connecting hinge 2	ACATTGTCAGTGAGATTCACTTTTTCTGCCAGTT
Connecting hinge 3	ACATTGAATAAGAACCACGGTTTTAGGAACAAC

Table S7. Primer pairs for construction of an expression vector for enzyme HG-XDH

Primer	**Sequence (from 5' to 3')**
F-*Nde*-Halo	ATATATATATCATATGGCAGAAATCGGTACTGGCTTTC
R-GCN4-TEV	GAGCACGTTTCAGAGCAGCCGGGTCGGCGATCGCGTTATC GCTCTGAAAG
F-TEV-GCN4	CTTTCAGAGCGATAACGCGATCGCCGACCCGGCTGCTCTG AAACGTGCTC
Rev-XDH-His-*Bam*HI	ATATATGGATCCTCAATGATGATGATGATGATGGCCGCCC TCAGG GCCGTCAAT

Supplementary References

1 Y. Amir, E. Ben-Ishay, D. Levner, S. Ittah, A. Abu-Horowitz and I. Bachelet, *Nat. Nanotechnol.*, 2014, **9**, 353-357.

2 T. A. Ngo, E. Nakata, M. Saimura, T. Kodaki and T. Morii, *Methods*, 2014, **67**, 142-150.

3 T. A. Ngo, E. Nakata, M. Saimura and T. Morii, *J. Am. Chem. Soc.*, 2016, **138**, 3012-3021.

4 J. E. Whitaker, R. P. Haugland and F. G. Prendergast, *Anal. Biochem.*, 1991, **194**, 330-344.

5 J. Han and K. Burgess, *Chem. Rev.*, 2010, **110**, 2709-2728.

6 E. Nakata, Y. Yukimachi, Y. Nazumi, Y. Uto, H. Maezawa, T. Hashimoto, Y. Okamoto and H. Hori, *Chem. Commun.*, 2010, **46**, 3526-3528.

7 T. Nguyen and M. B. Francis, *Org. Lett.*, 2003, **5**, 3245-3248.

8 R. V. Benjaminsen, H. Sun, J. R. Henriksen, N. M. Christensen, K. Almdal and T. L. Andresen, ACS *nano*, 2011, **5**, 5864-5873.

9 S. M. Douglas, A. H. Marblestone, S. Teerapittayanon, A. Vazquez, G. M. Church and W. M. Shih, *Nucleic Acids Res.*, 2009, **37**, 5001-5006.

10 B. Sander and M. M. Golas, *Microsc. Res. Tech.*, 2011, **74**, 642-663.